REPUBLIC OF TURKEY

YILDIZ TECHNICAL UNIVERSITY

GRADUATE SCHOOL OF NATURAL AND APPLIED SCIENCES

DEVELOPMENT OF SOL-GEL BASED ANTI-REFLECTIVE COATINGS FOR GLASSES USED IN PHOTOVOLTAIC SYSTEMS

Cennet YILDIRIM

MASTER OF SCIENCE THESIS

Department of Metallurgical and Materials Engineering

Production Program

Advisor

Assoc. Prof. Dr. Ali Erçin ERSUNDU

February, 2021

REPUBLIC OF TURKEY

YILDIZ TECHNICAL UNIVERSITY

GRADUATE SCHOOL OF NATURAL AND APPLIED SCIENCES

DEVELOPMENT OF SOL-GEL BASED ANTI-REFLECTIVE COATINGS FOR GLASSES USED IN PHOTOVOLTAIC SYSTEMS

A thesis submitted by Cennet YILDIRIM in partial fulfillment of the requirements for the degree of MASTER of SCIENCE is approved by the committee on 26.02.2021 in Department of Metallurgical and Materials Engineering, Production Program.

Assoc. Prof. Dr. Ali Erçin ERSUNDU

Yıldız Technical University

Advisor

Approved By the Examining Committee

Assoc. Prof. Dr. Ali Erçin ERSUNDU, Advisor
Yıldız Technical University _____

Asst. Prof. Dr. Hakan YILMAZER, Member
Yıldız Technical University _____

Prof. Dr. Sevim İŞÇİ TURUTOĞLU, Member
Istanbul Technical University _____

I hereby declare that I have obtained the required legal permissions during data collection and exploitation procedures, that I have made the in-text citations and cited the references properly, that I haven't falsified and/or fabricated research data and results of the study and that I have abided by the principles of the scientific research and ethics during my Thesis Study under the title of Development of Sol-Gel Based Anti-Reflective Coatings for Glasses Used in Photovoltaic Systems supervised by my supervisor, Assoc. Prof. Dr. Ali Erçin ERSUNDU. In the case of a discovery of false statement, I am to acknowledge any legal consequence.

Cennet YILDIRIM

Signature

Dedicated to my family and

dad who will live forever in my heart.

ACKNOWLEDGEMENTS

I would like to express my gratitude to my supervisor, Assoc. Prof. Dr. Ali Erçin ERSUNDU for his supervision, support, guidance, and encouragement during this study. I am also thankful to Assoc. Prof. Dr. Miray Çelikbilek ERSUNDU for her endless help during the entire period of my studentship. They trusted in me, gave me the chance to do independent research, and helped me get over every obstacle on the way.

I sincerely acknowledge the former and present members of YTU Glass Research Group for making this long journey fun.

This study would not be present without the support, endless understanding, and contribution of TENMAK-Boron Research Institute members; Assoc. Prof. Dr. Abdülkerim YÖRÜKOĞLU, Dr. Sedat SÜRDEM, M. Nasuh ARIK, and Orkun ELÇİN.

The study, which is the subject of this thesis, was conducted at the Department of Metallurgical and Materials Engineering of Yıldız Technical University. I am grateful to the Department of Metallurgical and Materials Engineering of Yıldız Technical University for giving me the opportunity to conduct a Master of Science study.

I am also thankful to my entire family for their regardless, lifelong support throughout my lengthy education, particularly to my parents Altın and Ali YILDIRIM. Especially, I would also like to thank my elder sister Hanife ARDAHANLI for her understanding and support.

Cennet YILDIRIM

TABLE OF CONTENTS

LIST OF SYMBOLS v

LIST OF ABBREVIATIONS vi

LIST OF FIGURES ix

LIST OF TABLES xii

ABSTRACT xiii

ÖZET xv

1 INTRODUCTION 1

1.1 Literature Review 1

1.2 Objective of the Thesis 3

1.3 Hypothesis 3

2 THEORETICAL INFORMATION 4

2.1 Energy Systems 4

2.2 Photovoltaic (PV) Systems 7

2.3 Cover Glasses Used in PV Systems 9

2.4 Anti-Reflective (AR) Coatings 12

2.5 Thin Film Deposition Methods 15

2.5.1 Chemical Vapor Deposition (CVD) Method 15

2.5.2 Physical Vapor Deposition (PVD) Method 16

2.5.3 Pulsed Laser Deposition (PLD) Method 17

2.5.4 Electrospinning Method 18

2.5.5 Sol-Gel Method 19

3 EXPERIMENTAL STUDIES 30

3.1 Starting Materials 30

3.2 Cleaning of Substrates 31
3.3 Preparation of Solutions and Coating Procedure 31
3.3.1 Determination of TEOS Ratio 33
3.3.2 Determination of Ammonia Solution Ratio 35
3.3.3 Determination of Aging Time 35
3.4 Characterization Studies 37
3.4.1 Optical Analysis 37
3.4.2 Phase Analysis 37
3.4.3 Morphological Analysis 37
3.4.4 Elemental Analysis and Depth Profiling 37
3.4.5 Topographical Analysis 38
4 RESULTS AND DISCUSSION **39**
4.1 Results 39
4.1.1 Optical Properties of Glass Substrates 39
4.1.2 Anti-reflective Coatings Deposited on Flat Glass Substrates 40
4.1.3 Anti-reflective Coatings Deposited on Prizma Patterned Glass Substrates 51
4.1.4 Anti-reflective Coatings Deposited on Sandy Patterned Glass Substrates 54
4.1.5 Comparison of Anti-reflective Coatings on Different Glass Substrates 57
4.2 Conclusions and Recommendations 58
REFERENCES **61**
PUBLICATIONS FROM THE THESIS **73**

LIST OF SYMBOLS

R	Alkyl
X	Anionic Group
°C	Degree Celcius
eV	Electron Volt
K	Kelvin
kV	Kilovolt
µm	Micrometer
ms	Millisecond
min	Minute
nm	Nanometer
n_i	Refractive Index of Substance
rpm	Revolutions Per Minute
v	Velocity of Light in a Medium
c	Velocity of Light in Vacuum

LIST OF ABBREVIATIONS

AFM	Atomic Force Microscopy
AR	Anti-Reflective
CVD	Chemical Vapor Deposition
EtOH	Ethanol
ITO	Indium Tin Oxide
MTES	Methyl Triethoxysilane
PLD	Pulsed Laser Deposition
PV	Photovoltaic
PVD	Physical Vapor Deposition
SEM	Scanning Electron Microscope
TEOS	Tetraethyl Orthosilicate
UV	Ultraviolet
XPS	X-ray Photoelectron Spectroscopy
XRD	X-ray Diffraction
XRF	X-ray Fluorescence Spectroscopy

LIST OF FIGURES

Figure 2.1 Renewable energy statistics as of 2019 5

Figure 2.2 Solar resurce map showing worldwide photovoltaic power potential as of 2019 6

Figure 2.3 The utilization rates of renewable energy sources in energy production in 2018 (left), the estimated utilization rates of renewable energy resources in 2050 (right) 6

Figure 2.4 The working principle of photovoltaic systems 7

Figure 2.5 Construction of a typical solar panel 8

Figure 2.6 The interaction of light with the cover glass surface 9

Figure 2.7 Estimated change in the transmission value of cover glasses with regard to years with and without AR coating 10

Figure 2.8 Change of thickness in cover glasses by years 11

Figure 2.9 The reflection of light on flat and patterned glass 11

Figure 2.10 The moth-eye (left) and its SEM image (right) 13

Figure 2.11 Schematic illustration of sunlights contacting with SiO_2 spheres deposited on the coating surface 14

Figure 2.12 Propagation of light rays through (left) a single layer film on substrate ($n<n_s$), (right) multilayer film on substrate 14

Figure 2.13 Microstructural arrays resulting from multiple reflections of light ... 15

Figure 2.14 (a) Schematic hot-wall CVD, (b) Low-pressure CVD 16

Figure 2.15 (a) Magnetron sputtering equipment and (b) diagram on the internal geometry used for the deposition of thin films of SiO_2 17

Figure 2.16 Schematic diagram of a typical laser deposition set-up 18

Figure 2.17 Electrospinning method 18

Figure 2.18 Illustration of synthesis steps of different products by sol-gel method (a) thin-film production from colloidal solution with different coating methods (b) powder production as a result of heat treatment of colloidal solution transformed into gel 21

Figure 2.19 Effect of pH on the structure of gel 24

Figure 2.20 Stages of spin coating method 26

Figure 2.21 Illustration of flow coating method 27

Figure 2.22 Illustration of spray coating method 27

Figure 2.23 Steps of dip coating method: (1) Immersion, (2) Start-up, (3) Deposition and Drainage, (4) Evaporation 29

Figure 3.1 Types of glass substrates along with their thicknesses 30

Figure 3.2 Cleaning of substrates in an ultrasonic bath using acetone (A), ethanol (E), and distilled water (W) 31

Figure 3.3 Preparation of solutions 32

Figure 3.4 Dip coating of prepared solutions 33

Figure 3.5 Heat treatment of as-deposited samples 33

Figure 3.6 Gelled solutions ready for coating 34

Figure 4.1 Transmittance spectra of different glass substrates a) 1.1 mm flat glass, c) 3.2 mm prizma glass, e) 3.2 mm sandy glass, b) 4 mm prizma glass, d) 4 mm sandy glass 39

Figure 4.2 Transmittance spectra of a) uncoated glass and coatings made by using b) acidic solution, c) basic solution, d) neutral solution (T: TEOS, E: Ethanol, H: Water, β: Basic, α: Acidic, Φ: Neutral) 40

Figure 4.3 Transmittance spectra of a) uncoated glass and coatings made by using different TEOS molar ratios b) 0.1, c) 0.25, d) 0.5, e) 0.75 (T: TEOS, E: Ethanol, H: Water, N: Ammonia) 41

Figure 4.4 The optimum ammonia ratio was determined by checking the optical transmittance value of glasses and also by evaluating its effect on gelation time. a) uncoated b) 0.05, c) 0.10, d)0.15, e) 0.20 (T: TEOS, E: Ethanol, H: Water, N: Ammonia) 43

Figure 4.5 Transmittance spectra of a) uncoated glass and coatings made after different aging periods b) 1 days, c) 3 days, d) 7 days, e) 10 days (T: TEOS, E: Ethanol, H: Water, N: Ammonia, A: Aging Time) 44

Figure 4.6 Transmittance spectra of uncoated glass along with single-sided (SS) and double-sided (DS) coatings after 1-day and 3-days aging (T: TEOS, E: Ethanol, H: Water, N: Ammonia, A: Aging Time) 45

Figure 4.7 SEM image of anti-reflective thin film coated flat glass surface under 500x magnification 46

Figure 4.8 Cross-sectional SEM image of anti-reflective thin film coated flat glass revealing the coating thickness 46

Figure 4.9 XRD result of anti-reflective thin film coated flat glass (a) and uncoated flat glass (b) 47

Figure 4.10 3D AFM topography image of anti-reflective thin film coated flat glass 48

Figure 4.11 (a) 2D AFM image of anti-reflective thin film coated flat glass, and (b) variation of roughness along the selected line 49

Figure 4.12 Variation of atomic % of elements with etching time 50

Figure 4.13 Transmittance spectra of prizma glasses and coatings made after different aging periods a) uncoated -3.2 mm, b) 3.2 mm-double sided-1 day, c) 3.2 mm-double sided-3 days, d) uncoated -4 mm, e) 4 mm-double sided-1 day, f) 4 mm-double sided-3 days (P: Prizma, DS: Double-Sided, A: Aging Time) 52

Figure 4.14 Optical microscope image of anti-reflective thin film coated prizma patterned glass surface under 50X magnification 52

Figure 4.15 SEM image of anti-reflective thin film coated prizma patterned glass surface under 500x magnification 53

Figure 4.16 XRD result of anti-reflective thin film coated prizma patterned glass 53

Figure 4.17 Transmittance spectra of sandy glasses and coatings made after different aging periods a) uncoated-3.2 mm, b) 3.2 mm-double sided-1 day, c) 3.2 mm-double sided-3 days, d) uncoated-4 mm e) 4 mm-double sided-1 day, f) 4 mm-double sided-3 days (S: Sandy, DS: Double-Sided, A: Aging Time) 55

Figure 4.18 Optical microscope images of anti-reflective thin film coated sandy patterned glass surface under 50X magnification 56

Figure 4.19 SEM image of anti-reflective thin film coated sandy patterned glass surface under 500x magnification 56

Figure 4.20 XRD result of anti-reflective thin film coated sandy patterned glass.. 57

LIST OF TABLES

Table 2.1 Refractive index values of different glass types 9

Table 2.2 The Advantages and disadvantages of sol-gel process 20

Table 2.4 The advantages and disadvantages of spin coating method 25

Table 2.5 The advantages and disadvantages of dip coating method 28

Table 3.1 Chemical composition (wt. %) of commercial glass substrates 31

Table 3.2 The molar ratio of acidic and basic solutions (T: TEOS, E: Ethanol, H: Water, β: Basic, α: Acidic, Φ: Neutral)..... 32

Table 3.3 Basic solutions with different TEOS amounts (T: TEOS, E: Ethanol, H: Water, N: Ammonia)..... 34

Table 3.4 Basic solutions with different ammonia solution amounts (T: TEOS, E: Ethanol, H: Water, N: Ammonia)..... 35

Table 3.5 Basic solutions aged for different durations (T: TEOS, E: Ethanol, H: Water, N: Ammonia, A: Aging Time) 36

Table 3.6 The different types of glasses obtained with solutions aged for different times (P: Prizma, S: Sandy, DS: Double-Sided, A: Aging Time)..... 36

Table 4.1 pH values of coated samples with respect to varying ammonia molar ratio 42

Table 4.2 Elemental analysis (wt%) of anti-reflective thin film coating on flat glass surface..... 49

Table 4.3 Depth profile etching results for different time periods 50

Table 4.4 Transmittance values of uncoated glasses along with double-sided (DS) coatings after 1-day and 3-days aging (T: TEOS, E: Ethanol, H: Water, N: Ammonia, A: Aging Time, S: Sandy, P: Prizma) 58

ABSTRACT

Development of Sol-Gel Based Anti-Reflective Coatings for Glasses Used in Photovoltaic Systems

Cennet YILDIRIM

Department of Metallurgical and Materials Engineering

Master of Science Thesis

Assoc. Prof. Dr. Ali Erçin Ersundu

Photovoltaic systems basically consist of different layers, and glass panels are located at the top layer of these structures. In order to increase the efficiency of photovoltaic systems, some improvements should be made on properties of glass panels. For this reason, different approaches have been proposed such as, preferring low iron containing glasses, utilizing thinner glasses, applying anti-reflective thin film coatings to the glass surface or using patterned glasses. Currently, flat soda-lime silicate glasses with low iron content are being widely used in photovoltaic systems. In recent years, parallel to the development of chemical tempering technology, the use of thinner glasses with high mechanical strength has also increased in glass industry. In addition, it is well known that solar energy efficiency can be increased in photovoltaic systems by applying anti-reflective coatings on glass panels. In the near future, with the use of anti-reflective coated thin patterned glasses in solar systems, further efficiency enhancements would be possible by increasing the light transmittance. However, the adaptation of anti-reflective coatings on patterned glasses is still in development. Therefore, the aim of this thesis is to increase the light transmittance of patterned and flat glasses by applying anti-reflective coatings and

to offer new alternatives to increase the efficiency of photovoltaic systems by making an up-to-date and original study. For this purpose, the optimization of anti-reflection coating parameters was made on 1.1 mm thick soda-lime silicate flat glasses. After determining the optimum parameters, anti-reflection coatings were applied on 3.2 and 4 mm thick commercial patterned glasses i.e., prizma and sandy. The optical, topographic, elemental, and structural properties of anti-reflective film coated glasses were examined by optical microscopy, UV-Vis spectrophotometry, SEM, AFM, XPS, and XRD techniques, respectively.

Keywords: Anti-Reflective Coating, Glass, Photovoltaic Systems, Sol-Gel

ÖZET

Fotovoltaik Sistemlerde Kullanılan Camlara Yönelik Sol-Jel Esaslı Yansıma Önleyici Kaplamaların Geliştirilmesi

Cennet YILDIRIM

Metalurji ve Malzeme Mühendisliği

Yüksek Lisans Tezi

Doç. Dr. Ali Erçin Ersundu

Fotovoltaik sistemler temel olarak farklı katmanlardan oluşmakta ve bu yapıların en üst katmanında cam paneller yer almaktadır. Fotovoltaik sistemlerin verimliliğinin arttırılabilmesi için cam panellerin özelliklerinde bazı iyileştirilmeler yapılmalıdır. Bu noktada, fotovoltaik sistemlerin verimini artırmak adına demir oranı daha düşük camların tercih edilmesi, daha ince camların kullanılması, yansıma önleyici ince film kaplamaların cam yüzeyine yapılması veya desenli camların kullanılması gibi farklı yöntemler uygulanabilmektedir. Bu nedenle, fotovoltaik sistemlerde yaygın olarak düşük demir oranına sahip soda-kireç silikat camları kullanılmaktadır. Son yıllarda kimyasal temperleme teknolojisinin gelişimine paralel olarak mekanik dayanımı yüksek ince camların kullanımında da artış başlamıştır. Bunlara ek olarak fotovoltaik sistemlerde kullanılan camlar üzerine yansıma önleyici kaplamalar yapılarak da güneş enerjisinden elde edilen verimde artış görülmüştür. Yakın gelecekte, solar sistemlerde yansıma önleyici kaplı ince desenli camların kullanımı ile ışık geçirgenliği arttırılarak daha fazla verim elde

etmek mümkün olacaktır. Ancak, desenli camlar üzerine yansıma önleyici kaplamaların adaptasyonu halen geliştirilme aşamasındadır. Bu nedenle, bu tez çalışmanın amacı desenli ve düz camlar üzerine uygulanacak yansıma önleyici (anti-reflektif) ince film kaplamalar ile camların ışık geçirgenliklerini arttırmak ve bu konuda güncel ve özgün bir çalışma yaparak fotovoltaik sistemlerin verimliliğini artırmak adına yeni öneriler sunmaktır. Bu amaç doğrultusunda yansıma önleyici kaplama parametrelerinin optimizasyonu 1,1 mm kalınlığındaki ticari soda-kireç silikat düz camlar üzerinde yapılmıştır. En uygun parametreler belirlendikten sonra yansıma önleyici kaplamalar 3,2 ve 4 mm kalınlığına sahip prizma ve sandy desenli ticari camlar üzerine uygulanmıştır. Kaplanan bu camların optik, topografik, minerolojik ve yapısal özellikleri sırasıyla optik mikroskop, UV-Vis spektrofotometre, SEM, AFM, XPS ve XRD cihazları ile incelenmiştir.

Anahtar Kelimeler: Yansıma Önleyici Kaplama, Cam, Fotovoltaik Sistemler, Sol-Jel

1
INTRODUCTION

1.1 Literature Review

World energy consumption is mainly based on non-renewable energy sources such as coal, natural gas, and oil [1]–[3]. In recent years, non-renewable energy sources have started to be depleted by their excessive use, and also the extensive consumption of non-renewable energy sources has caused serious environmental problems. For example, consuming fossil fuels produces a significant amount of carbon dioxide, which could accelerate the greenhouse effect and induce climate change [4], [5], [6]. Due to the above-mentioned reasons, the world must no longer rely on fossil-fuel-based energy sources. Therefore, the interest in renewable energy sources has started to increase, such as solar energy, wind energy, biomass, hydroelectric energy. Renewable energy sources are preferred because they are long-term clean energy sources [3], [7]. In short, renewable energy sources have started to play an important role in the world's future. Among different renewable energy sources, solar energy is especially one of the most promising candidates owing to its ubiquitous availability [8]. Thus, photovoltaic (PV) systems, directly converting sunlight energy to electricity, is one of the most important long-term clean energy solutions.

PV systems consist of multiple layers. The glass's main task in PV systems is to protect the solar cells and other layers [9], [10]. Glass material is of great importance in terms of light transmittance since sunlight's initial interaction is with the glass surface. Different glass types can be used in PV systems, such as fused silica, borosilicate, and soda-lime silicate. Soda-lime silicate glasses are widely preferred as they offer low cost advantage compared to other glass types [11], [12]. Increasing iron ratio in glass composition generally decreases the light transmittance. For this reason, glasses with low iron content are usually preferred in PV systems [13]. Another important parameter in terms of transmittance is the thickness of the glass.

Transmission decreases with increasing glass thickness [14], [15]. Different heat treatment processes have been developed to increase the durability of thin glasses, and thus the transmission has been increased thanks to the use of thinner glasses. However, the thickness of glasses has been limited. The reason why glass thickness cannot be further reduced is that thin glass strength cannot be increased by heat treatment methods, i.e. thermal tempering [16]. Recently chemical tempering process has started to be applied to thin glasses. In this way, the use of thinner glasses in PV systems has increased. Therefore, with use of thinner glasses higher transmittance values could be obtained for solar applications [17]–[19].

Sunlight is exposed to four different events on the glass surface: scattering, reflection, absorption, and transmission. The reduction of reflections on the surface is very important for the efficiency of PV systems [20]–[22]. In order to reduce the reflection rate in flat glasses, different patterns are given to the glasses. Hence, the efficiency of PV systems with the increase of light transmittance values are increased. For this reason, patterned glasses have started to be preferred in PV systems [23]–[25]. In addition, instead of just giving patterns to the glasses, a thin film coating on the surface of the glass can be used to reduce the reflection rate. Optimization studies of anti-reflective thin film coatings were carried out by paying attention to layer thicknesses, number of layers and refractive indices in thin film coatings to reduce reflection rate [26], [27]. The sol-gel method is widely preferred for the application of thin film coatings. In addition, the sol-gel process has different thin film coating methods such as spin coating, flow coating, spray coating and dip coating [28], [29]. Among these methods, the dip coating method is generally preferred for thin film coatings in terms of providing a homogeneous coating and being easily applicable to materials of different sizes and patterns [30]–[32].

Literature reviews show that patterned and thinner glasses having low iron content are potential candidate materials that can be used to increase light transmission in PV systems. In addition, the light transmittance value can also be improved with the application of anti-reflection coatings. However, these thin-film coatings are generally applied on flat glasses. Therefore, it is necessary to focus on the

development of anti-reflection coatings on patterned glasses to increase their potential in terms of light transmittance.

1.2 Objective of the Thesis

The widespread use of PV systems has become indispensable as an energy source. One of the factors affecting the efficiency of these systems is the glass surface that directly interacts with light at the top layer. Therefore, it is very important to increase the light transmission of cover glass in PV systems. Although different studies have been carried out to increase the light transmittance of cover glasses, to the best of my knowledge, no studies have been carried out on patterned glasses to enhance their optical properties for their integration in PV systems. Hence, this dissertation study aims to shed a light on properties of anti-reflective thin film coatings applied on patterned glasses. Therefore, within the objective of this thesis, optimization studies on pH, starting material ratios, and aging time was realized to understand their effect on anti-reflective coatings. Finally, optical, topographic, elemental, and structural properties of anti-reflective thin film coated patterned glasses were examined and compared with flat glasses.

1.3 Hypothesis

A patterned glass surface provides advantageous properties in terms of light transmittance. Therefore, one of the strategies to increase the efficiency of solar panels is the use of patterned glasses as cover materials to enable higher transmittance values. However, further improvement in transmittance values are still required in such applications. At this point, application of anti-reflective thin films to patterned glass surfaces are of great importance in order to meet the future demands from PV cover glasses. Previous studies on anti-reflective thin film coatings have not covered patterned glasses and only focused on flat glass surfaces. Therefore, as an original contribution to the field of study, this thesis work shows the effect of anti-reflective coatings on different commercial patterned glasses by investigating optical, topographic, elemental, and structural properties for the first time. As a result, possible use of patterned glasses in PV systems was evaluated.

2
THEORETICAL INFORMATION

2.1 Energy Systems

Over the years, the importance of energy has increased as a consequence of world's population growth and technological developments. Currently, world energy consumption is mainly based on fossil fuels [33], [34]. The reason why fossil fuels like coal, oil and natural gas are used so much is that they are easily accessible resources with currently available technology. Consuming fossil fuels has caused environmental damages producing a significant amount of carbon dioxide ultimately causing greenhouse effect and inducing the worldwide climate change [2], [35], [36]. The requirement of energy is increasing day by day as energy resources are depleted in an uncontrolled manner with the increasing population. In addition to this, limited fossil fuel resources make their long-term use difficult. Therefore, there is a need for clean, and sustainable resources for healthy living on earth [2]. In this perspective, interest in renewable energy sources, including wind energy, solar power, biomass, hydro power, geothermal energy has recently showed a dramatic increase [37], [38]. Among all renewable energy sources, solar energy steps forward due to sun's unlimited energy source. Figure 2.1 clearly reveals that solar energy has significantly more energy potential compared to other renewable energy sources.

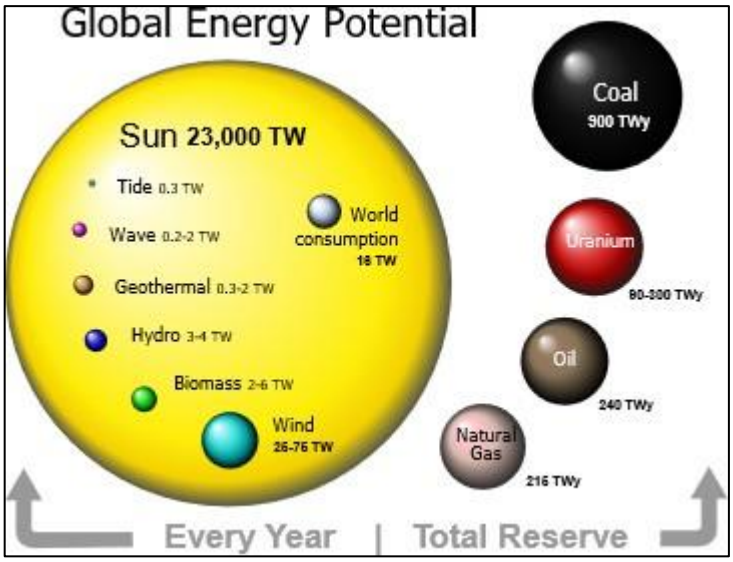


Figure 2.1 Renewable energy statistics as of 2019 [37]

At this point, photovoltaic (PV) systems have been developed to utilize solar energy. The main advantage of solar photovoltaic systems are that they are eco-friendly. Solar PV systems are used as an energy source in manufacturing and many other industries worldwide. Considering the costs of fossil fuels, demand for PV systems is increasing as it has become the most competitive alternative for electricity generation in residential, commercial applications, and many utility projects [39]. With the increase in its usage areas, PV systems have started to spread around the world. Particularly, with the increase in demand for high energy efficiency, the investments of countries in PV systems and the development studies they have made in these areas have started to increase [40]. As illustrated in Figure 2.2, this ratio has increased even more today, and solar energy has begun to become the main energy source in many countries.

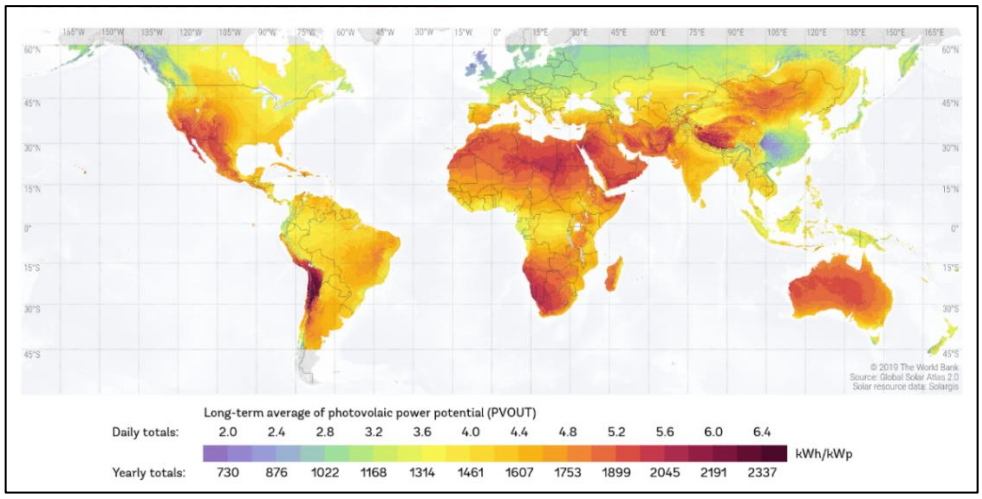


Figure 2.2 Solar resurce map showing worldwide photovoltaic power potential as of 2019 [1]

Figure 2.3 shows the worldwide photovoltaic power potential. It is expected that the ratio of solar PV systems which is about 9% in 2018 will increase to 69% in 2050 proving the high potential of PV systems among all renewables [41].

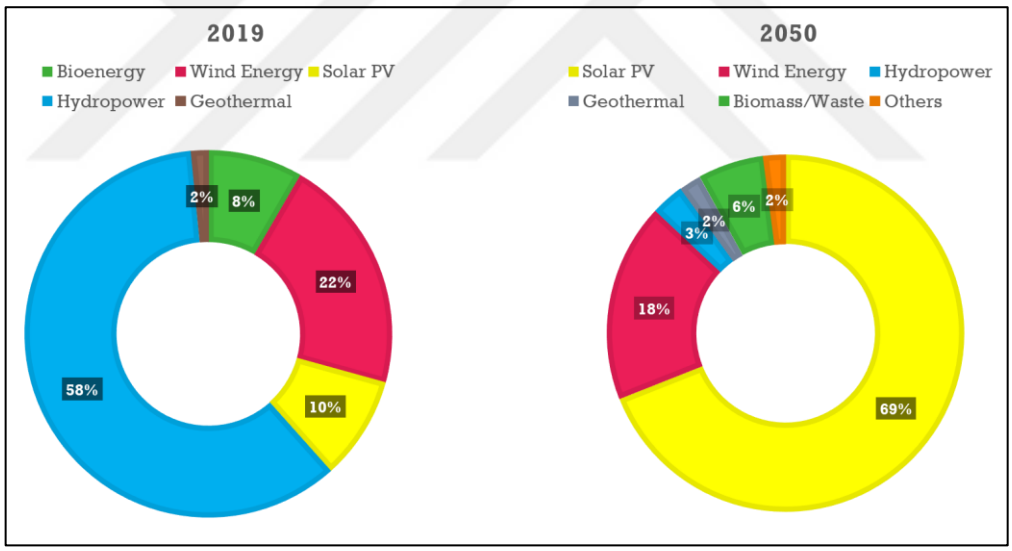


Figure 2.3 The utilization rates of renewable energy sources in energy production in 2019 (left), the estimated utilization rates of renewable energy resources in 2050 (right) [42]

Countries that anticipate this increase have already started to work on more efficient solar systems by making serious investments. As a first step, efforts were initiated on several issues such as, reducing the installation costs, reducing the

module fabrication costs, and more importantly increasing the overall efficiency of solar energy systems [43], [44].

2.2 Photovoltaic (PV) Systems

PV technologies play an important role in benefiting from solar energy. A solar cell, or photovoltaic cell generates electricity with the photovoltaic effect. Photovoltaic effect is a physical event in which sunlight is converted into electricity [45], [46]. Photons are formed when the sunlight hits the semiconductor surface and the electrons inside the atoms are released. Photon contains different amount of energy for each of wavelength in the solar radiation spectrum. When the photons come to the solar cell, some of it is reflected exactly, some of it is absorbed by the solar cell and some of it passes through the solar cell [47], [48]. Photons absorbed by the solar cell generate electricity. Figure 2.4 depicts the working principle of PV systems.

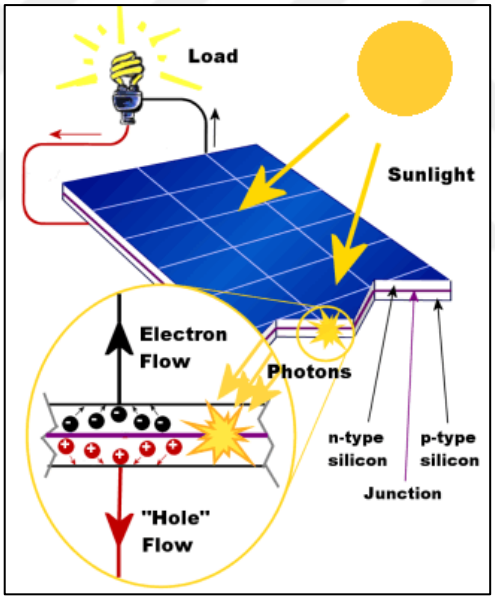


Figure 2.4 The working principle of photovoltaic systems [49]

Sunlight is formed from different colors as a result of the combination of high energy ultraviolet photons and low energy infrared photons in the visible wavelength range. Depending on specific bandwidth, each photovoltaic matter responds to a narrow gap of energies. The definition of the bandwidth is the amount of specific energy that is required to transfer an electron from a valance band filled with electrons to a free conduction band where electrons move easily. The unit of this is

electron volt, and it is defined by the eV symbol. The semiconductor n-type, which has several electrons in the conduction band, is attached to the dopant atoms to form an electrically negative material. P-type is a positive material that bonds to form electrons or vacancies in the valence band [50], [51]. The voltage source created with n and p types is shown in Figure 2.4. When the incident photons are absorbed, electrons and the voids move along the positive side of the joint towards the opposite side. As a result of this action, an electric current is generated. Electron separations occur due to the electric field generated in the p and n-type regions [3], [52]. As a consequence of this separation, a power output occurs between the contact ends of the photovoltaic panels. In summary, through the photons from the sun lights, the electrons in the n-type region are directed to the p-type region with electron deficiency, and the electric current is formed in this way [53]. As can be shown in Figure 2.5, photovoltaic systems consist of multiple layers.

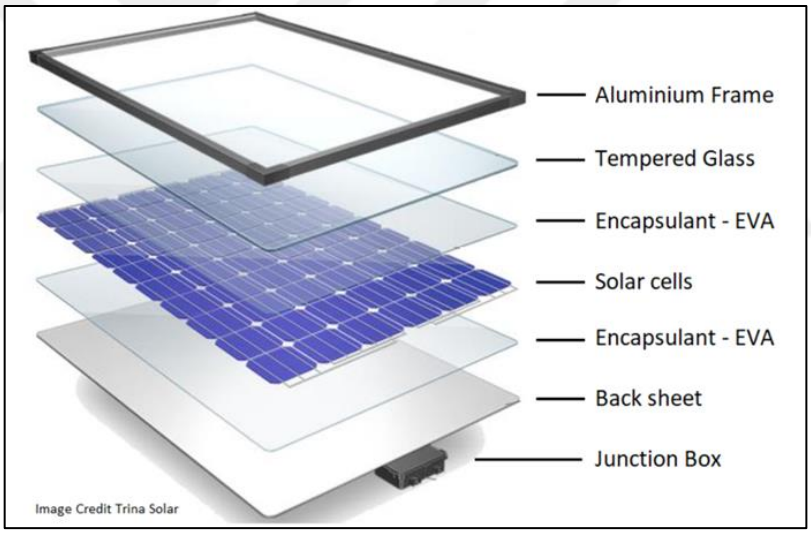


Figure 2.5 Construction of a typical solar panel [41]

Coating materials used in PV module systems are of great importance for optimum light capture and module life. In addition, the price of the module decreases according to the materials used. One of the PV module systems is cover glass. PV module prices vary according to the type of glass material used. Cover glass accounts for about 25% of the cost of Si thin film modules and about 10-15% of the cost of crystalline Si (c-Si) modules [13], [54].

2.3 Cover Glasses Used in PV Systems

In photovoltaic systems, the part where the sun's rays come into contact is the glass surface. Therefore, the properties of cover glass are important in order to increase the energy efficiency obtained from light. Many types of glass with different compositions are used in photovoltaic systems, such as fused silica, borosilicate glass, and soda-lime silicate glass, etc [13], [53]. The refractive index values of different glasses used in PV systems are given in Table 2.1. In general, transmission decreases with increasing refractive index value. Refractive index also determines the amount of light reflected when the material interface is reached [55]. Although, soda-lime silicate glasses have slightly higher refractive index values they are the most commonly preferred glasses in solar panels due their low cost [56].

Table 2.1 Refractive index values of different glass types [57]

Glass Types	Refractive Index (n)
Soda-Lime Silicate Glass	1.523
Borosilicate Glass	1.516
Fused Silica Glass	1.458

Four different events occur at the glass surface when the light comes into contact with the glass surface (see Figure 2.6). These are reflection, absorption, scattering, and transmission.

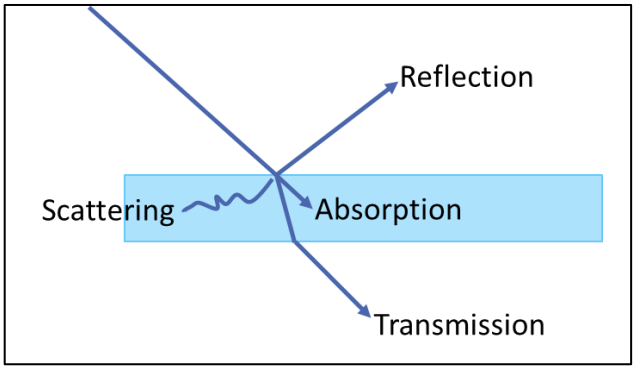


Figure 2.6 The interaction of light with the cover glass surface [58]

The transmission value varies according to the properties of cover glass. The transmission value of glasses used in PV systems today is approximately 91% and it is estimated that this value will reach to 92% in 2029 with the technological

improvements in glass industry [37], [59]. There are several methods to increase the light transmittance of a cover glass. One of these methods is to make anti-reflective coatings on the glass surface. Thanks to these coatings, today it is observed that the transmittance value of cover glasses can be increased approximately from 91% to 94% (see Figure 2.7). With continuous research and development studies on anti-reflective coatings, it is expected that the transmittance value of cover glasses will reach to almost 96% in 2029.

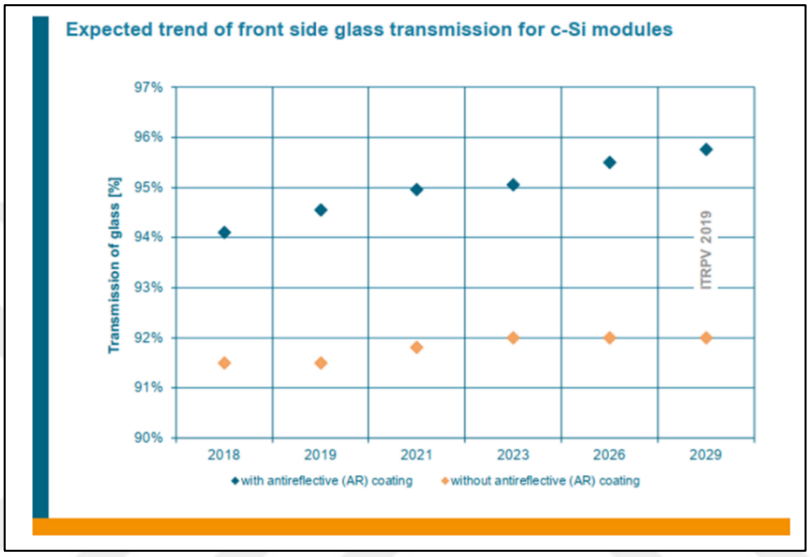


Figure 2.7 Estimated change in the transmission value of cover glasses with regard to years with and without AR coating [60]

A second way to increase the light transmission is to reduce the glass thickness. The greater the distance the light will travel, the less will it pass behind the material. Therefore, as the glass thickness increases, the transmittance value decreases. Figure 2.8 shows estimated change of thickness in cover glasses by years. As can be seen from Figure 2.8, cover glasses thicker than 3 mm were used in 2017, while glasses with a thickness between 2 mm and 3 mm are being used today. As of 2028, it is thought that glasses thinner than 2 mm will be used with advances in chemical tempering method which is widely used for strengthening of thin glasses. Chemical tempering will make the use of much thinner glasses possible in PV systems to yield higher transmittance values.

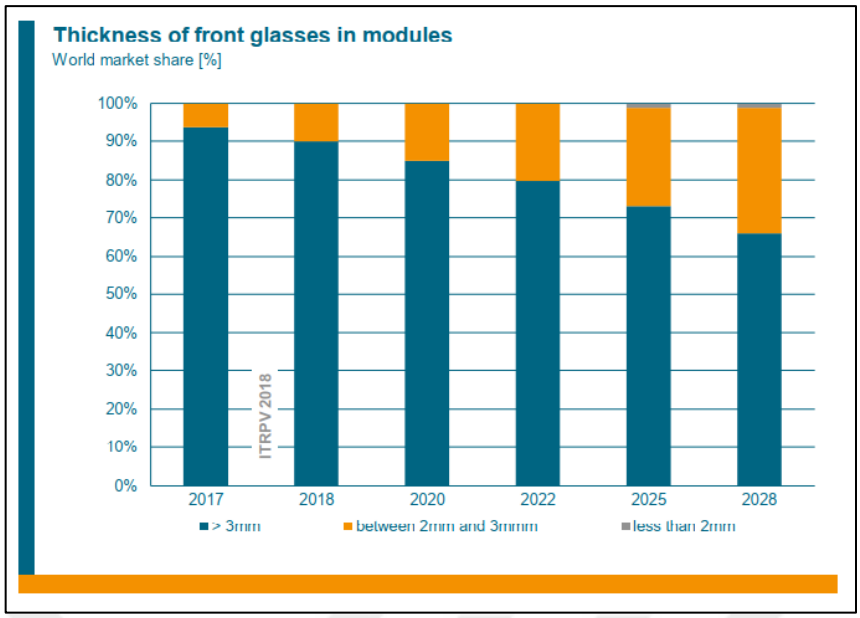


Figure 2.8 Change of thickness in cover glasses by years [15]

Thirdly, less reflection of incoming sun lights could be ensured by using patterned glasses. While the reflection is more in flat glasses, this rate is less in patterned glasses. This phenomenon is shown in Figure 2.9. Thanks to the pattern on the glass surface, the incoming rays pass through the material by performing a few refractions instead of reflecting directly. In flat glasses, this is quite the opposite.

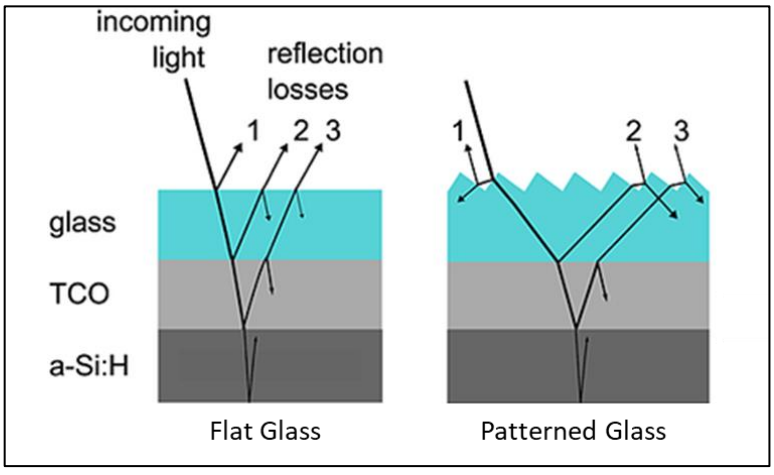


Figure 2.9 The reflection of light on flat and patterned glass [61]

Finally, the ratio of iron in the glass composition also has an effect on light transmittance. By changing the iron content in the glass composition, an improvement of 6% can be achieved in light transmission. Low-iron glasses generally consist of 0.01% iron (III) oxide (Fe_2O_3) in the composition [53]. Thanks

to these features, low-iron glasses are widely used in windows used in homes, especially solar panels, and other areas where clarity is desired.

2.4 Anti-Reflective (AR) Coatings

Anti-reflective coating (also called anti-glare coating) is a type of optical coating applied to the surface of a material to reduce reflection. Reflection is an optical phenomenon that occurs due to the change in the direction of light when the light is suddenly transferred to another medium. Optical interruption occurs in materials with a high refractive index [62], [63]. That is, incoming rays are scattered at certain angles. If scattering and absorption events are ignored, this phenomenon is called Fresnel reflection [64]. The ratio of light transmitted except the reflected rays shows the transmittance value [65]. Anti-reflective coatings have been developed to reduce the reflection rate and increase the transmittance value. Thanks to these coatings, a thin film with a lower refractive index is formed on the material surface, thereby increasing the transmission [24], [66]. The basic logic of anti-reflective coatings should be a dielectric coating with a refractive index lower than that of the substrate material. Reflection rate changes in relation to the value of refractive index [67]. Refractive index (n) is the amount of how much light slows down when it goes into a new medium, and refractive index (n) depends on two parameters: velocity of light in a vacuum (c) and velocity of light in a medium (v) (see Equation 2.1).

$$n = \frac{\mathbf{c}}{\mathbf{v}} \tag{2.1}$$

Anti-reflective coatings can be provided in many ways, for example, with thin films having a low refractive index or high porosity. While these films are designed, they were first inspired by moth eyes, as shown in Figure 2.10.

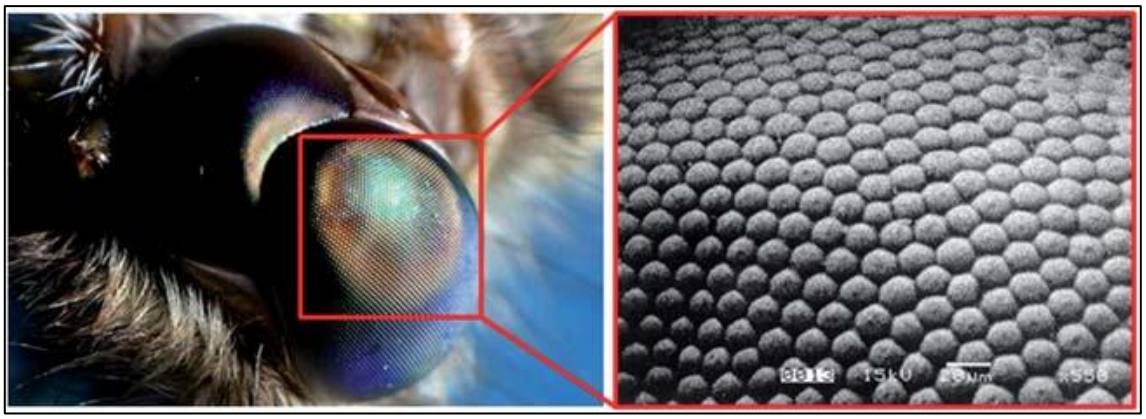


Figure 2.10 The moth-eye (left) and its SEM image (right) [68]

It has been determined that moth eyes have the highest light transmittance among other living things thanks to their porous structure [69]. In line with this finding, it has been observed that an increase in optical transmittance can be achieved with porous thin films [70]. These materials are generally sponge-like materials with nano-voids. It is well-known that the refractive index value decreases due to the increase in porosity [71], [72].

Anti-reflective coatings must have some certain properties. First of all, the coating should cover a wide wavelength range. This range may vary according to usage areas [24], [73]. Secondly, the coatings must be able to adhere with the substrate material and must be suitable for the environment to be used in. For this reason, it is important that the coatings do not only offer good anti-reflective properties but also have different properties such as hydrophobicity [17], [74]. In addition to these features, the production cost of the coatings should be reasonable.

For anti-reflective purposes different coating materials can be used. For instance, metal oxides or fluorides such as TiO_2, ZnO, Al_2O_3, indium tin oxide (ITO), Ta_2O and MgF_2 are generally preferred [75]. Furthermore, polymer-based materials such as polystyrene (PS), polymethyl methacrylate (PMMA), poly dimethylsiloxane (PDMS), and polyethylene terephthalate (PET) can be used [76]. Silicon oxide-based materials are also generally applied including tetraethyl orthosilicate (TEOS) and methyl triethoxysilane (MTES). The end product always remains in the form of SiO_2 in silicone-based anti-reflective coatings [77]. As shown in Figure 2.11, it accumulates on the surface.

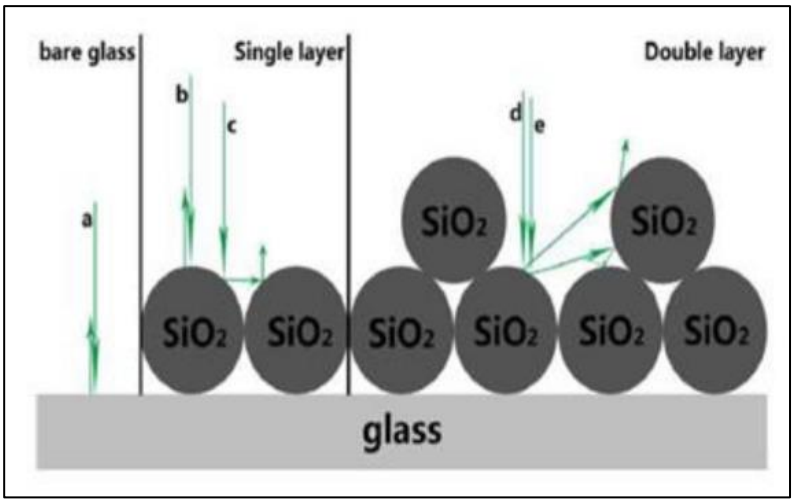


Figure 2.11 Schematic illustration of sunlights contacting with SiO_2 spheres deposited on the coating surface [44]

Antireflective coatings can consist of single or multiple layers as illustrated in Figure 2.12. While the refractive index of the surface material and coating is important in coatings made in single layers, the refractive index of each layer in multilayer coatings is of great importance on transmittance.

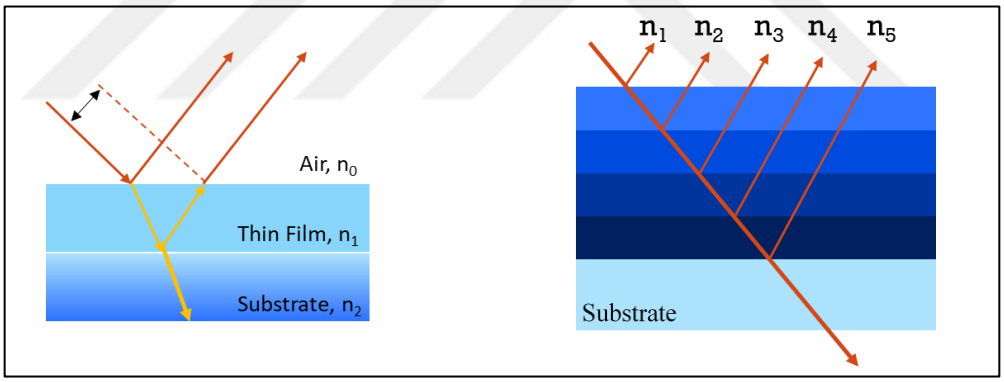


Figure 2.12 Propagation of light rays through (left) a single layer film on substrate ($n<n_s$), (right) multilayer film on substrate [57], [78]

It is also very important whether the surface of the substrate material used in anti-reflective coating studies is rough or not. Theoretically, when the light comes to the surface, it will be trapped in the gaps caused by the roughness on the surface, as shown in Figure 2.13.

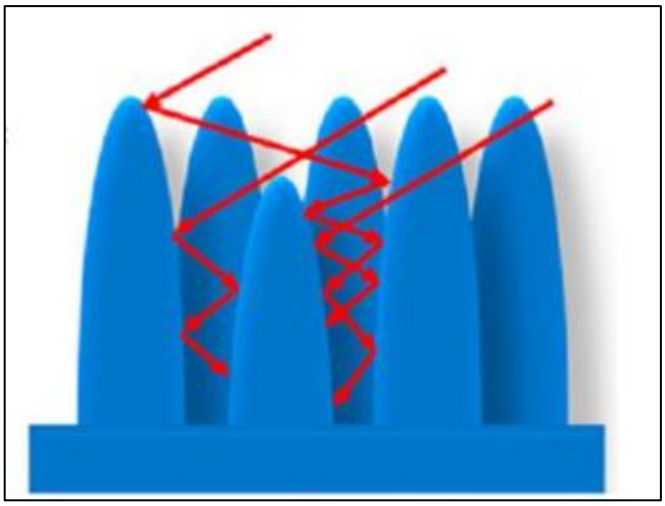


Figure 2.13 Microstructural arrays resulting from multiple reflections of light [79]

For this reason, the etching process can be performed using hydrogen peroxide (H_2O_2) or hydrogen fluoride (HF) on glass surfaces [80].

2.5 Thin Film Deposition Methods

A wide variety of thin film deposition methods are available for AR coatings such as, chemical vapor deposition (CVD), physical vapor deposition (PVD), sol-gel synthesis, chemical solution deposition, and electrospinning method.

2.5.1 Chemical Vapor Deposition (CVD) Method

Chemical vapor deposition (CVD) is a deposition method used to produce high-performance thin-film coatings or solid materials under vacuum [81]. In this method, a chemical reaction takes place between organometallic or halide compounds and other gases. [82]. There are two different CVD methods, as shown in Figure 2.14. The hot-wall system is a conventional example of CVD. The low-pressure system is a system used for small parts.

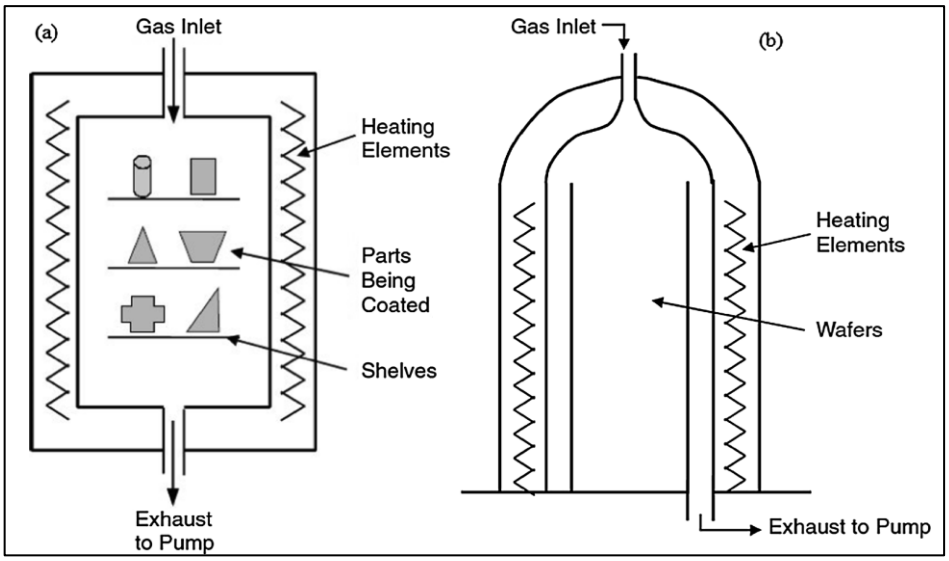


Figure 2.14 (a) Schematic hot-wall CVD, (b) Low-pressure CVD [83]

Since the final product obtained in the CVD technique has a frosted appearance, the transmittance value, which is important for optical applications, decreases [84]. Besides, usage areas are limited due to the fact that it cannot be applied to very large parts.

2.5.2 Physical Vapor Deposition (PVD) Method

It is also possible to make anti-reflective coatings using physical vapor deposition (PVD) technique [85]. With this coating method, extremely pure and high-performance coatings can be provided. The basic logic in the PVD method is to spray atoms at a certain distance from a source to a material to be coated by evaporation. In Figure 2.15, the PVD system used for anti-reflective coatings is shown. SiO_2 magnetron is used as the coating material, and the surface is sprayed over magnetron.

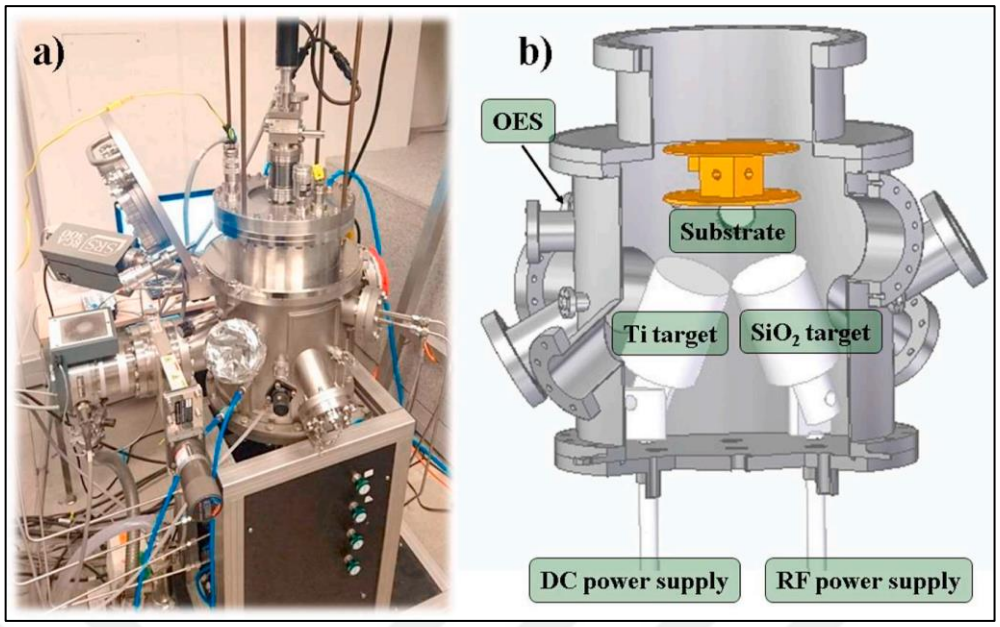


Figure 2.15 (a) Magnetron sputtering equipment and (b) diagram on the internal geometry used for the deposition of thin films of SiO_2 [86]

Although this coating method is used in thin-film coatings, it is usually not preferred for anti-reflective coatings due to the cost of the technique and the need for a high vacuum or suitable pressure environment [87].

2.5.3 Pulsed Laser Deposition (PLD) Method

The pulsed laser deposition (PLD) method is one of the vapor deposition methods performed by sending a very powerful laser beam onto the material to be coated [88]. The general setup for PLD is shown schematically in Figure 2.16. This system generally hits the target with a 45° laser beam under a very high vacuum. The ions or atoms detached from the target are deposited on the material to be coated, thus obtaining thin-film coatings.

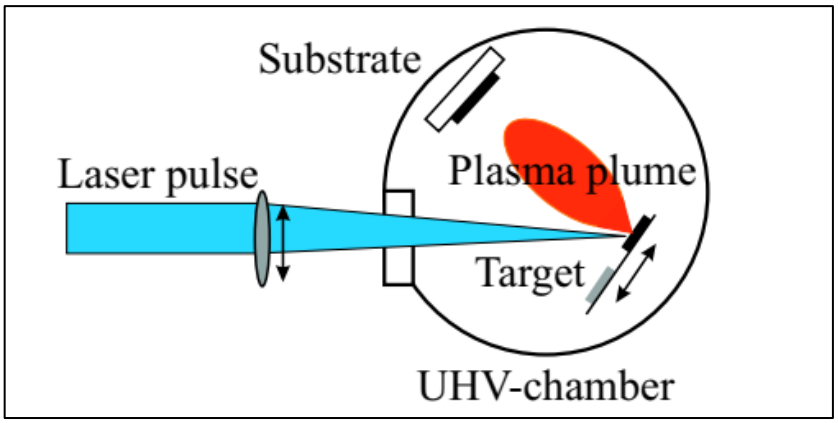


Figure 2.16 Schematic diagram of a typical laser deposition set-up [89]

The most significant disadvantage of this coating method is that it is costly compared to other methods [90]. Therefore, it has a very limited usage area and less preferred. In addition, the physical phenomena of laser-target interaction and film growth are highly complex in this method.

2.5.4 Electrospinning Method

Electrospinning is a versatile technique commonly used to produce ultra-thin nanofibers [91]. In general, it works with the logic of producing fibers with nanometer diameters by leaving a polymer solution under the influence of an electrostatic field.

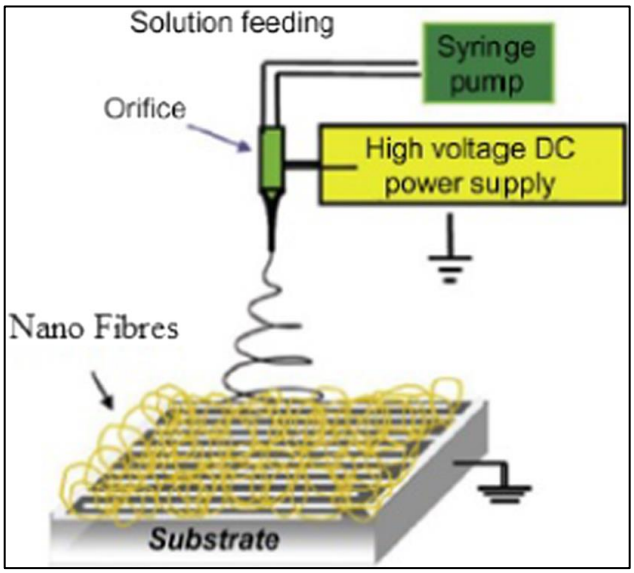


Figure 2.17 Electrospinning method [92]

As shown in Figure 2.17, the coating is made by spraying the prepared solution from a needle tip to the surface of the material to be coated in an electrostatically applied environment. Although this method offers the opportunity to cover large surfaces, it causes problems due to the very low coating speed [93]. The coating thickness increases due to the slow coating speed. The cost of the equipment used is also high.

2.5.5 Sol-Gel Method

Compared to CVD, PVD, PLD, and electrospinning methods, the sol-gel method is cheaper and easier to adapt to large scale and mass production. The most important feature of the sol-gel method is that it is suitable for preparing films with common and inexpensive methods that require less equipment, such as dipping and rotating before the solution is gelling [94]. Besides, an advantage of the sol-gel method compared to other methods is that the properties of the coated film such as pore volume, pore size, and surface area can be completely controlled.

The sol-gel process includes the formation of colloidal suspensions (sol) consisting of solid particles in a liquid phase and then three-dimensional solid inorganic network structures (gel) in a continuous liquid phase. Sol can be defined as a stable suspension of solid particles in the liquid. In the sol-gel technique, a solution (sol) is usually prepared to contain metal alkoxide, water, and alcohol, this sol is gelated, and the solvents are removed. Solid particles suspended in the liquid form the sol. These particles, called colloids, are 1-1000 nm in size and do not collapse to the bottom thanks to intermolecular Van Der Waals forces and electrical repulsion forces, which are much greater than the gravitational force. The gel is the name of the molecule expanding in solution and reaching macro size. It is a continuous intermediate phase between the solid and liquid phases. The sol-gel method is used literally as an abbreviation for solution-gelation. It was first discovered in the 1840s. Since the 1930s, it has been widely studied [95]. As shown in Table 2.2, the sol-gel method has many advantages and disadvantages. This is of great importance in increasing the reasons for being preferred.

Table 2.2 The Advantages and Disadvantages of Sol-Gel Process [96]

ADVANTAGES	DISADVANTAGES
The chemical direction of the method can be controlled.	Expensive starting materials used.
Providing better homogeneity compared to raw materials	Excessive loss of material in practice
Ability to obtain powder sizes below micron	Using chemicals harmful to health
Suitable for the production of special products such as thin films	Residual carbon can be included in the structure.
Energy-saving - Ability to process at low temperatures	The presence of residual hydroxyl in the structure
Possibility to obtain new properties and materials	Long processing time
The films prepared are pure.	The sol is getting old.
Minimizing air pollution	
Simple process	
Can be applied to large surfaces	
No interaction with the prepared environment	
Allowing metal doping	

There are three components used in the sol-gel method. These are the starting material, solvent, and catalyst. The chemical reactant containing the M cation in the sol or gel is called the chemical starting material. Chemical conversions of starting materials are quite complex. In the sol-gel method, the choice of a stable and low toxic starting material is crucial as the precursor plays a crucial role in film formation. As shown in Figure 2.18, multiple steps can be performed using the sol-gel method. Sol-gel process is applied by selecting the appropriate step according to the purpose.

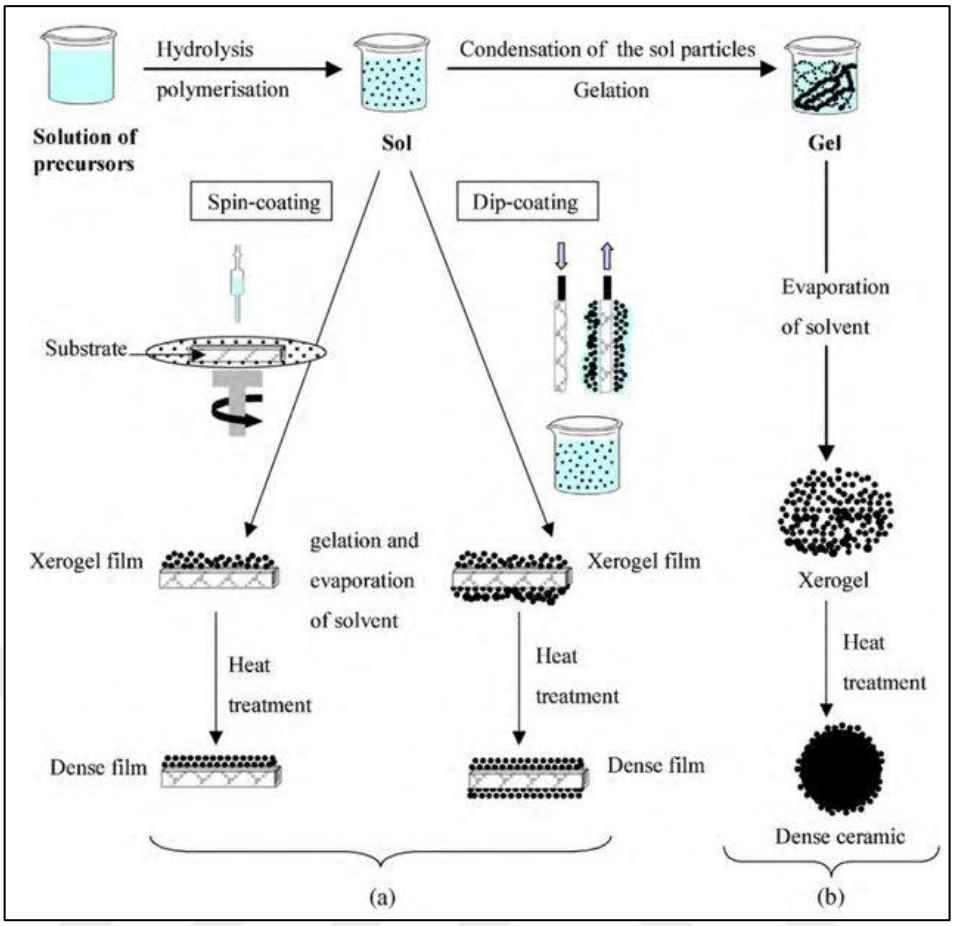


Figure 2.18 Illustration of synthesis steps of different products by sol-gel method (a) thin-film production from colloidal solution with different coating methods (b) powder production as a result of heat treatment of colloidal solution transformed into gel [97]

There are two main groups of starting materials, metallic salts and alkoxides. The general formula for metallic salts is:

$$M_mX_n \tag{2.2}$$

Here M metal, X is anionic group, m, and n are stoichiometric coefficients. Using metallic salts in aqueous solutions is inexpensive but difficult to control the reaction method of sol production. The general formula for alkoxides is shown as follows:

$$M(OR)_n \tag{2.3}$$

The combination of the alcohol group n with the cation M is shown in the formula. Due to the high electronegative OR group they contain, the participation of metal alkoxides in the reaction is quite high. Differences in physical properties are

achieved by changing the alkyl groups in the metal alkoxide. The choice of water or organic solvent as a solvent in the sol-gel process depends on the starting material. The solution chemistry of the two groups of starting materials is different from each other [21], [84].

In the sol-gel method, water, alcohols, and alkyl halides are used as solvents. Water is generally used in ceramics synthesized by the sol-gel method and some oxides. Besides, alcohols are generally used to dissolve metal alkoxides. They are formed by bonding a hydroxide (OH) group to an alkyl (R) molecule and are designated as R-OH. The alcohol to be used as a solvent is selected according to the properties of the alkoxide. Alcohols are polar molecules. On the other hand, alkyl halides are obtained by halogen bonding to alkyl groups and denoted as R-X. Here R represents the alkyl group, and X represents halogens. They are polar molecules, just like alcohol. However, their density varies according to the halogen size. The larger the halogen, the higher the density. They are prepared by the reaction of alkyl halides, alcohols, and hydrogen halides [98], [99].

Catalysts, the third component used in the sol-gel method, are added to the mixture to accelerate the reaction. It increases the speed of the reaction. They come off without reacting. There are two types, acid and base catalysts.

The basis of the sol-gel process is the combination of starting materials such as metal alkoxide solutions or metal powders with solvents and catalysts in certain proportions to form a sol. The mixing of this sol at certain temperatures takes place in many successive chemical reactions. A network is formed by the electrochemical interaction of the particles' surface charges resulting from the reactions, and this network grows and reaches all points in the system to form a gel. The sol-gel process consists of several steps. Solution preparation is the first of these steps. In this step, a homogeneous solution is prepared due to the reaction carried out by mixing various starting materials with suitable solvents. Sol-gel steps after solution preparation:

- Hydrolysis Reaction

$$M(OR)_4\ H_2O \rightarrow HO\text{-}M(OR)_3 + ROH. \quad (2.4)$$

This reaction can continue to convert all OR groups to OH groups, depending on the amount of water and catalyst. Factors affecting the rate of hydrolysis are water amount, catalyst type, solvent concentration, and temperature.

- Condensation Reaction

Two groups of hydrolyzed groups are connected by oxygen bridges;

$$(OR)_3 - OH + HO - M(OR)_3 \rightarrow (OR)_3 - O\,M(OR)_3 - H_2O \quad (2.5)$$

If either of the two groups is not hydrolyzed;

$$(OR)_3 - OR + HO - M(OR)_3 \rightarrow (OR)_3 - O - M(OR)_3 + RHO \quad (2.6)$$

takes place in the form [100].

Thus, the products of the reaction are subjected to hydrolysis. The products undergo condensation reactions again.

- Polymerization

Large molecules can be obtained by condensation. This stage, which results in an increase in the molecular chain length, is called polymerization. In the sol-gel method, polymerization occurs in three stages:

• The formation of particles as a result of polymerization of monomers,

• The growth of these particles,

• The particles are bound in a chain and then thicken and gel by forming a network structure in the liquid.

The factors affecting the polymerization steps are pH, temperature, reaction time, concentration, catalyst and its amount, aging temperature, and aging time.

- Gelation

As the last step of the sol-gel method, the growth of gel clusters due to clustering and condensation of polymers is called gelation. Gels are viscoelastic substances composed of weak or strong bonds, bound together in micron size, and have pores [101].

The sol-gel synthesis is based on the hydrolysis, polymerization, condensation of molecular precursors, nucleation, and gelation. Each of these processes is affected by the pH value, aging and mixing time, the proportion of added materials, ambient temperature, and many other parameters [102]. Especially the pH balance is very important. The basic or acidic nature of the solution affects the formation of a colloidal structure and, consequently, gelation. It can be seen from Figure 2.19 that more colloidal structure is formed in basic solutions. At the same time, the gelation time varies according to the alkalinity level.

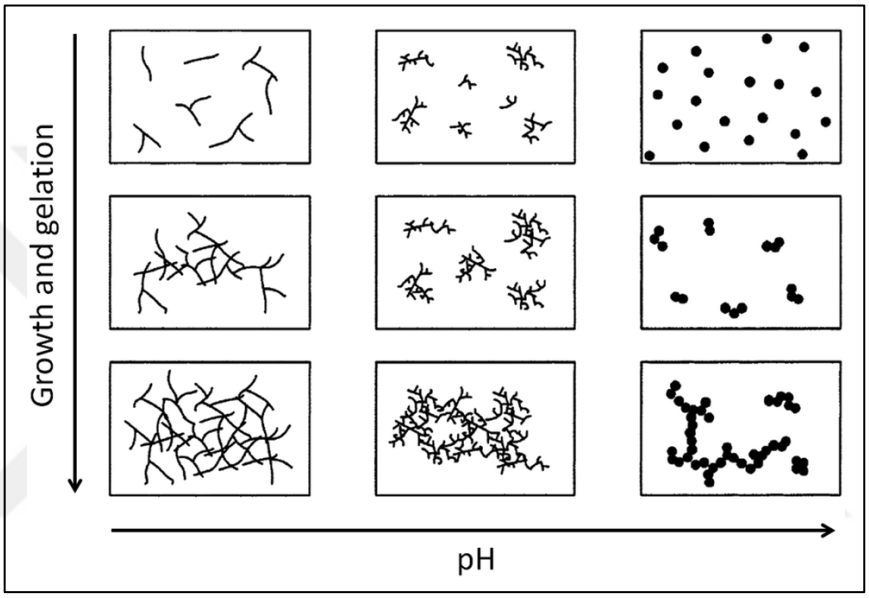


Figure 2.19 Effect of pH on the structure of gel [103]

In addition to this, the sol-gel process has different thin-film coating methods such as spin coating, flow coating, spray coating, and dip coating. Generally, the optical quality of the coatings obtained by using one of the sol-gel coating methods on glass is high.

Spin Coating Method

In the first stage of spin coating, some liquid is poured on the surface. In the second stage of rotation, the liquid flows out of the surface due to the centrifugal force. When the spin-up device begins to spin, the solution covers the entire substrate surface, the highest rotation speed is reached in the spin-off stages, and the solution becomes thinner and becomes a coating. At the end of the rotation, no excess liquid remains on the surface. In the most important stage, the evaporation step, the film

takes its final form. An advantage of this process is that the film formed on the surface is evenly distributed. Therefore, the film thickness is homogeneous across the surface. The centrifugal force that causes the fluid on the pad to flow radially outward and the friction force acting in the opposite direction is effective in the thickness being homogeneous [104].

The film thickness depends on the viscosity of the solution and the spin speed. Besides the centrifugal force acting as the film rotates, the gravitational force is negligible since it is tiny. So, it can be said that there is only the centrifugal force in the thinning of the film. As the rotation speed increases, the film thickness decreases. The advantages and disadvantages of the coating method are given in Table 2.4.

Table 2.3 The advantages and disadvantages of spin coating method [20]

ADVANTAGES	**DISADVANTAGES**
The devices are much cheaper than vacuum evaporation and splash coating devices.	It is an efficient method only for symmetrical carriers.
Even large pads can be covered with a small amount of sol.	It is not easy to keep clean.
Sol loss is low.	However, flat samples can be used for coating.
It is a speedy technique. It saves time.	It is not easy to coat large carriers homogeneously.
Ideal for multilayer applications.	In case of rapid evaporation of the solvent, homogeneous coatings cannot be obtained, and the solvent that evaporates late may not dissolve the material.
It is possible to obtain all types of commercial equipment.	

The spin coating operate is comprised of four stage. These are deposition, spin-up, spin-off, and evaporation, respectively. These stages are shown in Figure 2.20. Description of each step is given below.

• Deposition: the substrate surface is coated by an excess amount of sol to get entirely wet surface.

• Spin-up: the bottom layer is accelerated up to the final desire speed for the selected time; hence, due to the centrifugal force effect, sol spreads all over the surface and excess amount of the sol is thrown from the surface.

• Spin-off: In this step bottom layer spins at a constant speed. viscous forces make the fluid becomes thinner, and edge effects of sol are usually observed because of the high speed of spin.

• Evaporation: Coating thinning mechanism is dominant and at this stage of the process almost all solvents evaporate simultaneously since they are highly volatile. Conversion from sol to gel begins after the solvent has evaporated.

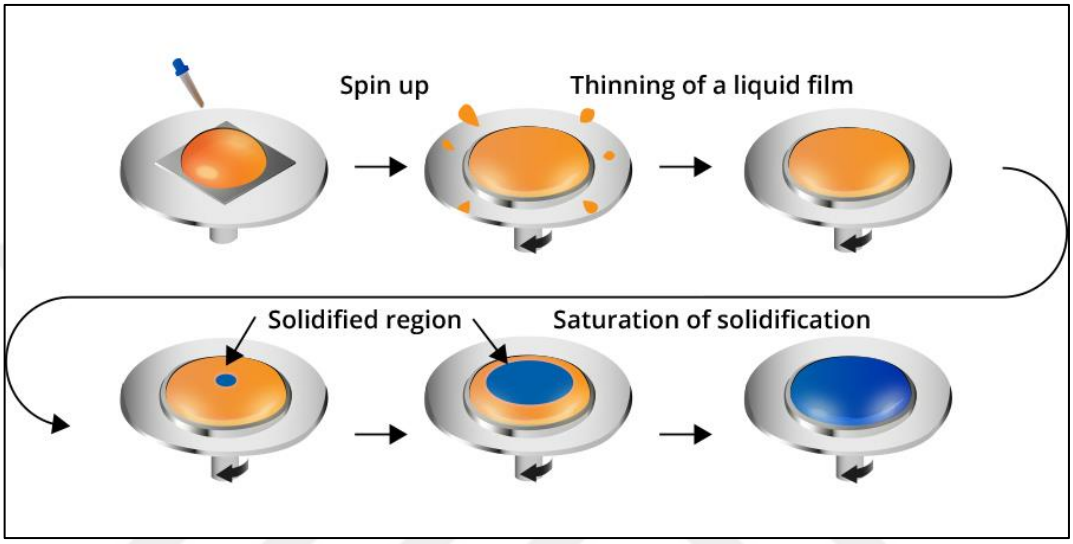


Figure 2.20 Stages of spin coating method [105]

Flow Coating Method

In the flow coating system, as shown in Figure 2.21, the solution is applied gradually to the surface of the material to be coated [106]. The coating thickness is affected by the inclination angle of the substrate, the viscosity of the coating fluid, and the solvent evaporation rate. The biggest advantage of this coating is that it provides a homogeneous coating on non-planar surfaces by spinning. Thanks to this spinning process, the coating thickness is increased from top to bottom of the substrate. Today, the flow coating method is widely used for hard coating automotive glass from polycarbonate.

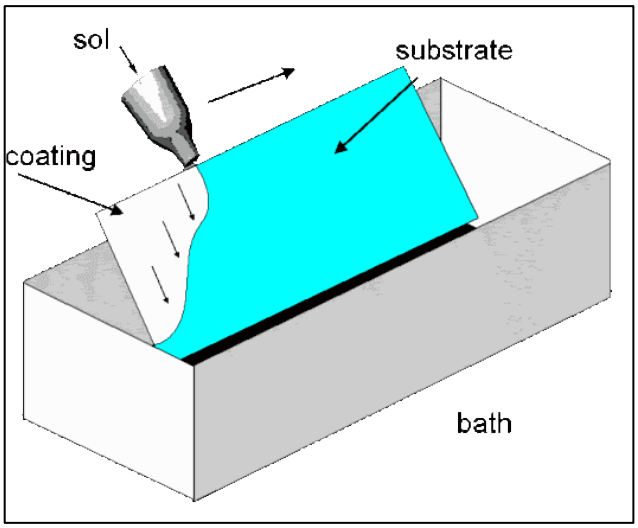


Figure 2.21 Illustration of flow coating method [107]

Spray Coating Method

In this method, diluted solution of sol is sprayed onto the sample surface (see Figure 2.22). Spray pressure and rate of scanning are directable parameters for the coating. The wetting of the surface of substrate and the boiling point of the sol are important deposition factors [7]. Spray coating makes it possible to deposit on complex surfaces since process of spray coating is fast and it requires low amount of sol. Therefore, it is an efficient and widely used coating technique in the industry.

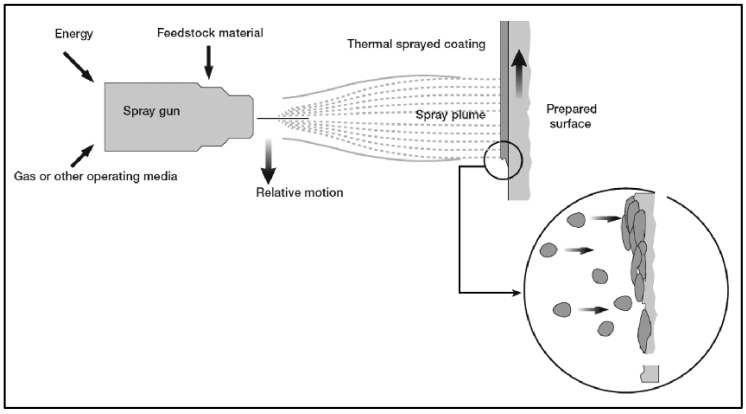


Figure 2.22 Illustration of spray coating method [32]

Dip Coating Method

The dip coating method is the process of immersing the surface to be coated in an environment where temperature and atmospheric conditions can be controlled and withdrawing at the same speed [108].

The forces acting in film formation are:

- Frictional force between pad moving upward and left

- Gravitational force

- Surface tension force created by the left attachment to the base

- Inertial force of the boundary layer of the liquid adhering to the substrate

- Separating and joining pressure (important for films thinner than 1μm)

- Surface tension profile

The coated surface is called underlay. It can be of flat-panel, cylinder, or complex geometric shapes. Glass, silicon, etc. can be used as base materials. Speed control is important, and vibration should be very low in order to obtain a smooth and homogeneous coating. Dip coating is preferred because of being cheaper and easier than other thin-film coating methods. Detailed advantages and disadvantages are given in Table 2.5.

Table 2.4 The advantages and disadvantages of dip coating method [109]

ADVANTAGES	DISADVANTAGES
It is possible to coat any shape and size of the samples.	Too much solution required for large litter
A smooth surface is obtained, and thickness can be controlled.	It requires masking when the single-sided coating is desired since it is covered on both sides of the base.
It is easy to keep the number of additives to a minimum.	Not a very good method for multilayer systems due to corner contamination
Its cost is cheap.	
A large number of samples can be coated at the same time.	
It is not very sensitive to solvent or solution properties.	
It can be worked in a controlled atmosphere.	
It is possible to make multilayer coatings.	
Contamination can be kept to a minimum.	

Dip coating consists of four stages as follows (see Figure 2.23):

i. Immersion: the substrate is dipped in the coating solution at a constant speed.

ii. Hold time: the immersed substrate is held on the sol for a certain time to allow the sol particles to penetrate.

iii. Deposition: substrates are removed from the solution at a constant speed without vibration. In this process, the sol is coated on the entire surface of the substrate. The film thickness depends on the dipping speed, the content of the solution, and the viscosity of the liquid. Increasing speed decreases thickness of film or vice versa.

iv. Evaporation: evacuation of excess sol and evaporation of solvent from the deposited film. If the solvent is volatile like alcohol, the evaporation process has already started during the deposition stage [110].

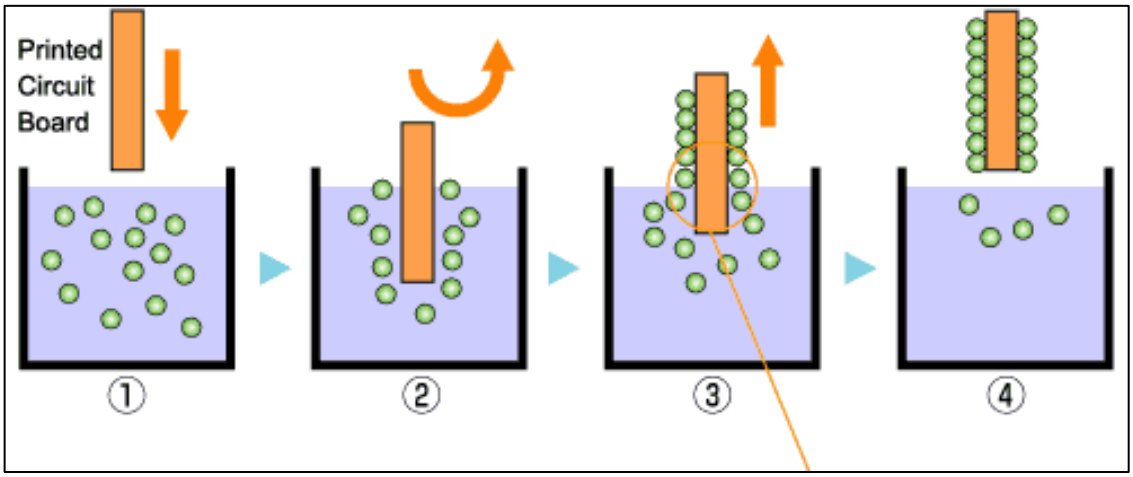


Figure 2.23 Steps of dip coating method: (1) Immersion, (2) Start-up, (3) Deposition and Drainage, (4) Evaporation [111]

3
EXPERIMENTAL STUDIES

In this thesis work, effect of anti-reflective coatings on soda-lime silicate glasses are investigated in terms of structural, topographic, morphological, and optical properties for different coating conditions. The optical transmittance of thin films is investigated using a UV-Vis spectrophotometer. Phase characterizations are performed by thin-film XRD technique. The morphology of anti-reflective coatings is observed by optical microscopy and SEM analysis. The elemental distribution and thickness of the thin films are determined by XPS. Finally, the roughness of the anti-reflective coating surface is observed by AFM analysis.

3.1 Starting Materials

Commercial glasses supplied from Şişecam were used in this study as substrates. Two different low-iron containing patterned glasses, prizma and sandy, having two different thickness values as 3.2 and 4 mm were selected and compared with conventional 1.1 mm flat glasses (Figure 3.1). The elemental compositions of studied glasses were determined using a Rigaku Primus II X-Ray Fluorescence (XRF) spectrometer and the compositional information is given in Table 3.1.

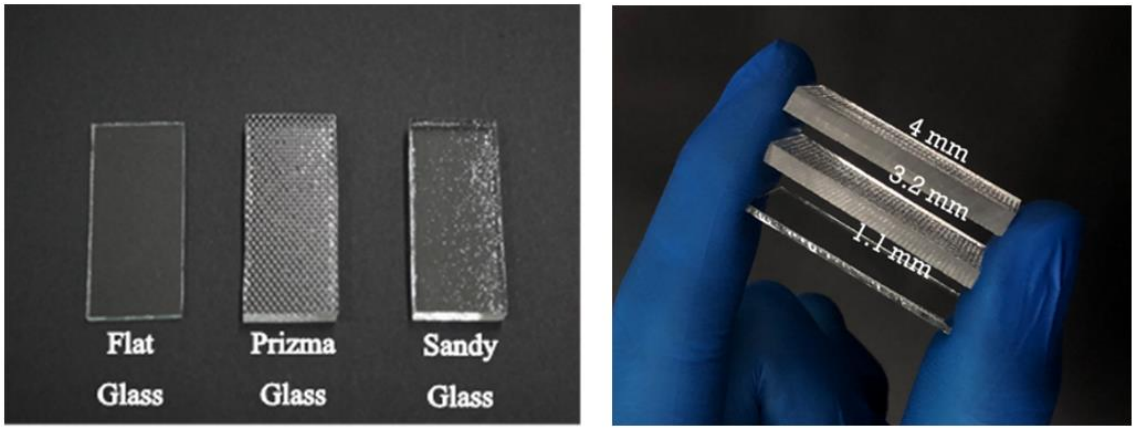


Figure 3.1 Types of glass substrates along with their thicknesses

Table 3.1 Chemical composition (wt. %) of commercial glass substrates

	SiO_2	Na_2O	CaO	MgO	Al_2O_3	Fe_2O_3	Others
Flat Glass	71.7	13.8	8.1	4.4	1	0.60	0.4
Sandy Glass	72.3	13.4	8.4	4.4	1	0.07	0.4
Prizma Glass	72.3	13.4	8.4	4.4	1	0.07	0.4

For the sol-gel preparations tetraethyl orthosilicate (TEOS) (Sigma Aldrich, ≥99.0%), ethanol (Merck, absolute for analysis), ammonia solution (Merck, 32%), HCl (Merck, 37%), and distilled water were used.

3.2 Cleaning of Substrates

Different types of glasses were cut to 35 x 15 mm in size using a diamond glass cutter. Surface conditions of substrate glasses used in the thesis have great importance in terms of the consistency and reliability of the data produced. Therefore, before applying anti-reflective coatings, glasses were held in each acetone, ethanol, and distilled water for 10 minutes, respectively using an ultrasonic bath (see Figure 3.2). Afterwards, glass substrates were allowed to dry in a sealed container at 25 °C for 1-3 days.

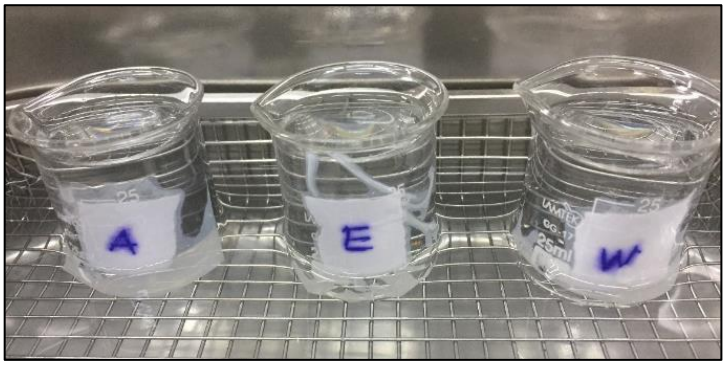


Figure 3.2 Cleaning of substrates in an ultrasonic bath using acetone (A), ethanol (E), and distilled water (W)

3.3 Preparation of Solutions and Coating Procedure

Different orthosilicate solutions were prepared using TEOS, ethanol, and H_2O. The molar ratios of these starting materials were determined after examining the work

of Zhang et al. [48]. Ammonia solution and HCl were then added dropwise to make these solutions basic and acidic, respectively (see Table 3.2).

Table 3.2 The molar ratio of acidic and basic solutions (T: TEOS, E: Ethanol, H: Water, β: Basic, α: Acidic, Φ: Neutral)

Sample Code	TEOS	Ethanol	Water	Ammonia solution	HCl
$T_1E_{1.8}H_{18}$-β	1	1.8	18	added dropwise until pH reaches to 10	-
$T_1E_{1.8}H_{18}$-α	1	1.8	18	-	added dropwise until pH reaches to 2
$T_1E_{1.8}H_{18}$-Φ	1	1.8	18	-	-

In addition, a third neutral solution was also prepared as a reference without adding any acidic or basic materials by keeping the ratio of TEOS, water, and ammonia constant. The prepared solutions were stirred for 30 minutes at 30 °C at 300 rpm using magnetic stirrers (see Figure 3.3).

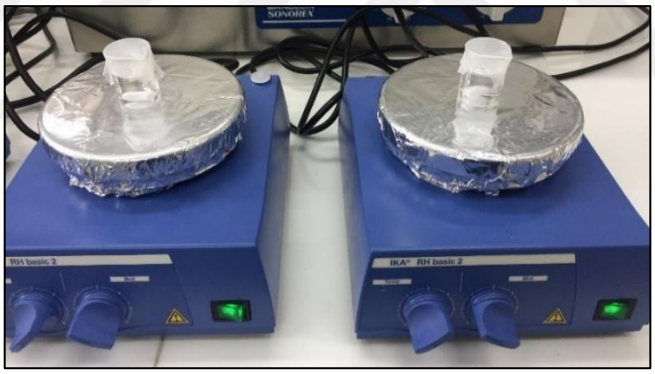


Figure 3.3 Preparation of solutions

During solution preparation, pH was monitored and measured as 5. Afterwards, HCl and ammonia solutions were added to the orthosilicate solutions dropwise until their pH becomes 2, and 10, respectively. Each prepared solution was then stirred for extra one hour at 60 °C at 300 rpm. When the solutions was observed to turn into a jelly form, they were coated on 1.1 mm thick flat soda-lime silicate glass substrates for solution optimization studies using a withdrawal rate of 100 mm/min (see Figure 3.4). The thin films were deposited as double-sided and single-sided coatings on glass substrates to investigate the effect of coating side.



Figure 3.4 Dip coating of prepared solutions

Afterwards, coated samples were dried in air for 10 minutes at room temperature. Finally, as-deposited samples were heat-treated at 500 °C for one hour to remove excess ammonia, ethanol, and water (see Figure 3.5). After comparing the performance of basic and acidic solutions, basic solution was selected for further studies as it shows better optical performance. In addition, faster gelation was achieved by adding ammonia to the solution. It was observed that the gelation time was prolonged if ammonia solution was not used.

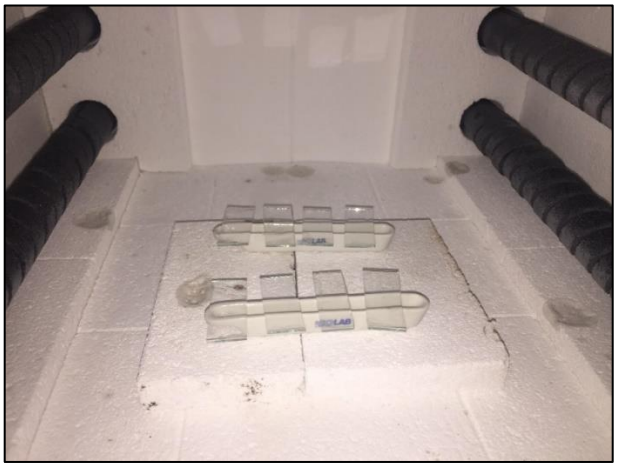


Figure 3.5 Heat treatment of as-deposited samples

3.3.1 Determination of TEOS Ratio

After selecting basic solution for further studies, firstly the effect of TEOS rate in the solution was investigated. Molar amount of remaining ingredients was kept

constant, while increasing the TEOS ratio according to the work of Es'kin et al. [94]. Therefore, basic solutions having four different compositions with following TEOS molar ratios: 0.10, 0.25, 0.50, and 0.75 were prepared (see Table 3.3).

Table 3.3 Basic solutions with different TEOS amounts (T: TEOS, E: Ethanol, H: Water, N: Ammonia)

Sample Code	TEOS	Ethanol	Water	Ammonia Solution	pH
$T_{0.10}E_8H_{1.5}N_{0.2}$	0.10	8	1.5	0.2	11.43
$T_{0.25}E_8H_{1.5}N_{0.2}$	0.25	8	1.5	0.2	11.40
$T_{0.50}E_8H_{1.5}N_{0.2}$	0.50	8	1.5	0.2	11.16
$T_{0.75}E_8H_{1.5}N_{0.2}$	0.75	8	1.5	0.2	10.92

The prepared solutions were stirred at room temperature for 4 hours at 300 rpm. At the end of 4 hours, the pH values were measured (see Table 3.3), and each solution was subjected to aging for 3 days in order to realize the gelation. After gelation was completed (see Figure 3.6), the coating process was applied to 1.1 mm thick flat soda-lime silicate glasses.



Figure 3.6 Gelled solutions ready for coating

Afterwards, the anti-reflective thin film coated samples were annealed at 500 °C for one hour. The purpose of annealing is to ensure that the coating adheres to the surface and prevents it from being easily removed from the surface in case of any impact or contact with water. The effect annealing was already examined at different temperatures in different studies [67], [96], [112]. The most important factor in determining the temperature is the glass transition temperature. The

important thing is to be able to apply the heat treatment process without damaging the glass form or causing softening in the glass. Therefore, in this work 500 °C that is below the glass transition value of commercial soda-lime silicate glasses was preferred as the annealing temperature. The optimum TEOS ratio was determined by checking the optical transmittance value of glasses.

3.3.2 Determination of Ammonia Solution Ratio

After choosing the ideal TEOS ratio for basic solution, the optimum amount of ammonia solution (NH_4OH) was determined the second step. Therefore, molar amount of remaining ingredients was kept constant, while varying the NH_4OH ratio (see Table 3.4). The solution preparation, coating and heat-treatment procedures were identical with TEOS determination studies. The optimum ammonia ratio was determined by checking the optical transmittance value of glasses and also by evaluating its effect on gelation time.

Table 3.4 Basic solutions with different ammonia solution amounts (T: TEOS, E: Ethanol, H: Water, N: Ammonia)

Sample Code	TEOS	Ethanol	Water	Ammonia Solution	pH
$T_{0.25}E_8H_{1.5}N_{0.05}$	0.25	8	1.5	0.05	9.98
$T_{0.25}E_8H_{1.5}N_{0.10}$	0.25	8	1.5	0.1	10.24
$T_{0.25}E_8H_{1.5}N_{0.15}$	0.25	8	1.5	0.15	10.32
$T_{0.25}E_8H_{1.5}N_{0.20}$	0.25	8	1.5	0.2	10.75

3.3.3 Determination of Aging Time

After determining the TEOS and NH_4OH ratios of basic solution, effect of aging time was investigated as the third step. For the determination of aging time, the ratio of all starting materials were kept constant according to the optimum TEOS, EtOH, H_2O, and NH_4OH amounts and the solutions were stirred at room temperature for 4 hours. Afterwards, the solution was left for 1, 3, 7, and 10 days of aging periods in order to realize the gelation. pH values were measured after each aging time was completed (see Table 3.5).

Table 3.5 Basic solutions aged for different durations (T: TEOS, E: Ethanol, H: Water, N: Ammonia, A: Aging Time)

Sample Code	Aging Time (days)	TEOS	Ethanol	Water	Ammonia Solution	pH
$T_{0.25}E_8H_{1.5}N_{0.2}$-1A	**1**	0.25	8	1.5	0.2	11.43
$T_{0.25}E_8H_{1.5}N_{0.2}$-3A	**3**	0.25	8	1.5	0.2	10.32
$T_{0.25}E_8H_{1.5}N_{0.2}$-7A	**7**	0.25	8	1.5	0.2	9.81
$T_{0.25}E_8H_{1.5}N_{0.2}$-10A	**10**	0.25	8	1.5	0.2	9.55

Upon completing the aging process, samples were subjected to annealing at 500 °C for one hour. Optimum aging time was determined according to the optical transmittance results.

As a consequence of the optimization studies realized using 1.1 mm thick flat soda-lime silicate glass substrates, the optimum molar ratio of anti-reflective solution was determined as follows: TEOS:EtOH:H_2O:NH_4OH = 0.25:8:1.5:0.2. Afterwards, the coatings were deposited on prizma and sandy glasses to investigate the effect of anti-reflective coatings on low-iron patterned glasses. Solutions were subjected to two different aging periods as 1 and 3 days. Subsequently, they were coated using dip-coating method at a dipping speed of 100 mm/min. This speed was determined as ideal according to similar studies reported in the literature [56], [107]. Solutions were applied to the substrates as single-sided and double-sided coatings. Further studies were conducted using double-sided coatings as they show higher transmittance values compared to single-sided coatings. The samples obtained as a result of the experiments are named as shown in Table 3.6.

Table 3.6 The different types of glasses obtained with solutions aged for different times (P: Prizma, S: Sandy, DS: Double-Sided, A: Aging Time)

Sample Code	Glass Type	Thickness (mm)	Coating Side	Aging Time (days)
P3.2-DS-1A	Prizma	3.2	Double Sided	1
P4-DS-3A		4		3
S3.2-DS-1A	Sandy	3.2		1
S3.2-DS-3A		4		3

3.4 Characterization Studies

3.4.1 Optical Analysis

The optical transmission spectra of coated glass substrates were recorded using a PG instruments T80+ UV-Vis spectrophotometer in the spectral range of 360-700 nm with 1 nm spectral resolution.

3.4.2 Phase Analysis

Phase analysis of coated glass substrates was realized using a PANalytical/Empreyan X-Ray Diffraction (XRD) device operated in thin film mode using a Cu $K_{\alpha 1}$ source at a wavelength of 1.540562 Å. XRD spectra was collected in the 2θ range from 5° to 75° with a step size of 0.02°.

3.4.3 Morphological Analysis

QUANTA 400F field emission scanning electron microscope (SEM) was used to investigate the morphology of prepared samples. SEM analysis was operated under 15kV voltage. Samples were gold plated to provide conductivity before the SEM investigations. Samples were cut and their cross-sectional examination was realized to determine the thickness of thin films.

3.4.4 Elemental Analysis and Dept Profiling

X-Ray photoelectron spectroscopy (XPS) analysis is an elemental and quantitative analysis method based on obtaining characteristic X-ray spectra depending on excitation from all kinds of solid material (pellet, thin-film, powder) excited with a single wavelength. Thermo Scientific / K-Alpha brand X-Ray photoelectron spectrometer device with Al K_{α} as an X-ray source was used. For the XPS analysis 200 kV X-ray power with 400 μm X-ray spot size was set up. For each area, 200.0 eV pass energy was used for a high-resolution regional scan. To remove each layer, Ar ion was bombarded with 1 kV energy at 50 ms dwell time. After general XPS survey was completed, the depth profile analysis was used to confirm the thickness of coating. 1000 eV ion energy and 2 mm raster size were applied in the depth profile step for 2200 seconds.

3.4.5 Topographical Analysis

Atomic force microscopy (AFM) was used to collect information about surface topography and surface roughness for anti-reflective coatings on flat glass substrates. In this study, AFM measurements were realized in tapping mode by using Nano Surf-Nanite-B version 2.2 CSM Instrument with a coverage area of 77 μm^2 and using time/Line as 1s.

4
RESULTS AND DISCUSSION

4.1 Results

4.1.1 Optical Properties of Glass Substrates

Transmittance spectra of glasses supplied from Şişecam to be used as substrates in anti-reflective coating process are shown in Figure 4.1.

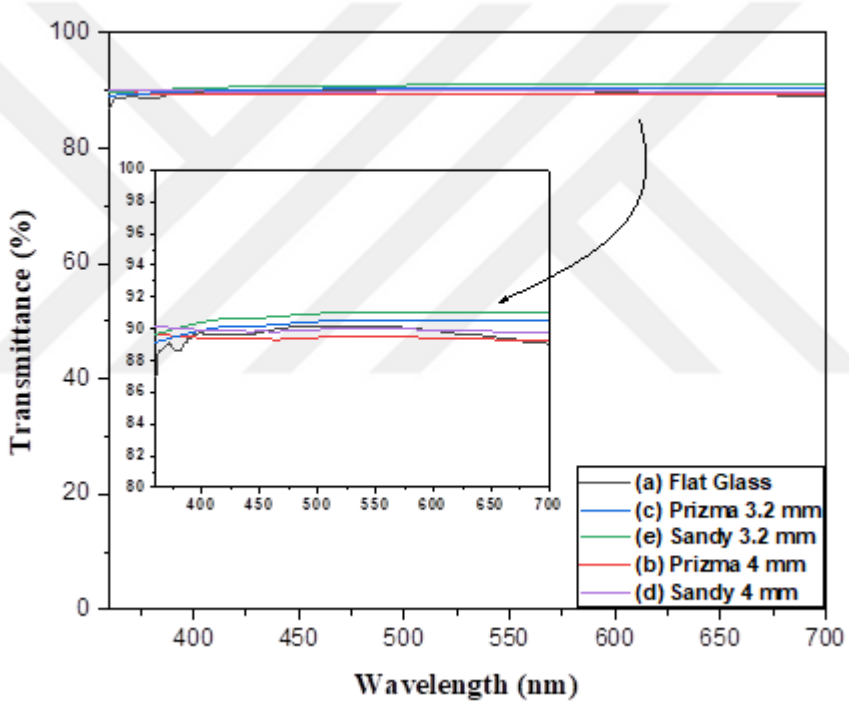


Figure 4.1 Transmittance spectra of different glass substrates a) 1.1 mm flat glass, c) 3.2 mm prizma glass, e) 3.2 mm sandy glass, b) 4 mm prizma glass, d) 4 mm sandy glass

The average visible transmittance of 1.1 mm flat glass was determined as 90.5%, while for 3.2 mm and 4 mm prizma and sandy patterned glasses the average visible transmittance values were detected around 91% and 90%, respectively. As can be seen from Figure 4.1, there is no significant transmittance difference in selected

glasses. This result shows that all commercial glasses selected as substrate materials have high visible transmittance and are suitable for anti-reflective coatings.

4.1.2 Anti-reflective Coatings Deposited on Flat Glass Substrates

Anti-reflective coatings are primarily deposited on flat glass substrates in order to optimize the sol-gel parameters and coating conditions.

Firstly, the effect of pH of prepared solutions on optical performance of anti-reflective thin film coatings are examined. Therefore, optical transmittance of three different coatings obtained by the deposition of HCl added acidic solution (T1E1.8H18-α), NH_4OH added basic solution (T1E1.8H18-β) and neutral solution (T1E1.8H18-Φ) on flat glass substrates are investigated and the visible transmittance spectrum of each sample along with uncoated glass substrate is shown in Figure 4.2.

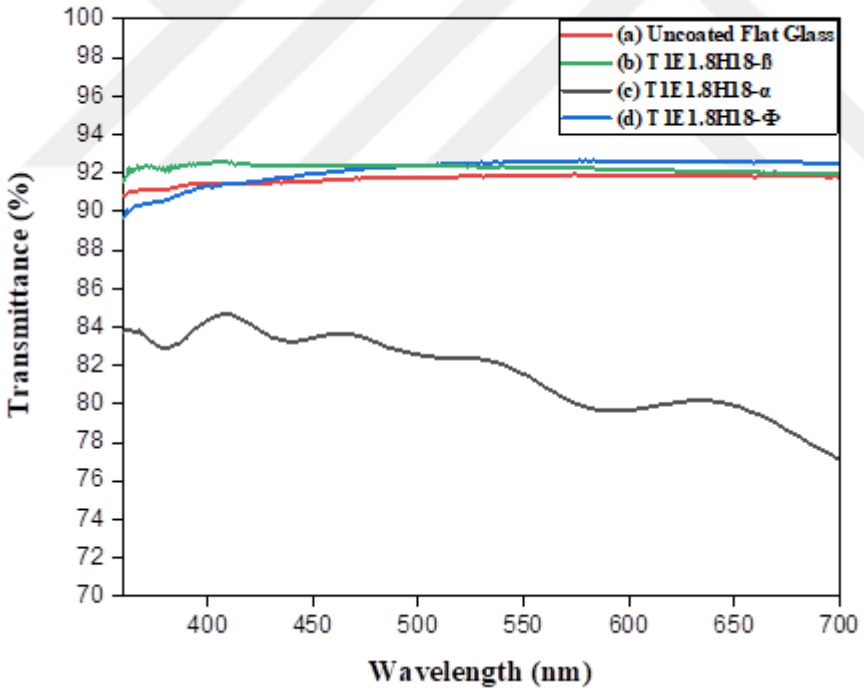


Figure 4.2 Transmittance spectra of a) uncoated glass and coatings made by using b) basic solution, c) acidic solution, d) neutral solution (T: TEOS, E: Ethanol, H: Water, β: Basic, α: Acidic, Φ: Neutral)

As can be clearly seen from Figure 4.2, when compared to uncoated glass the transmittance values obtained by using acidic solution showed a significant decrease, while no dramatic change was observed in the transmittance values of basic and neutral solutions. It is also noteworthy to mention that the addition of ammonia to the solution improved the reaction rate and shortened the gelation time. Therefore, basic solution was preferred for further studies.

Secondly, in order to observe the effect of TEOS amount on optical performance of anti-reflective thin film coatings, the molar ratio of TEOS was adjusted by keeping the ammonia solution ratio constant. Therefore, molar ratio of TEOS was varied between 0.10 and 0.75 to prepare different basic solutions. According to the previous experience, the ratio of ethanol and water was adjusted since the increase in the ratio of ethanol and water increased the material hydrolysis time and gelation time. The visible transmittance spectra of coatings with different TEOS ratios applied on flat glass substrates are shown and compared with uncoated glass substrate in Figure 4.3.

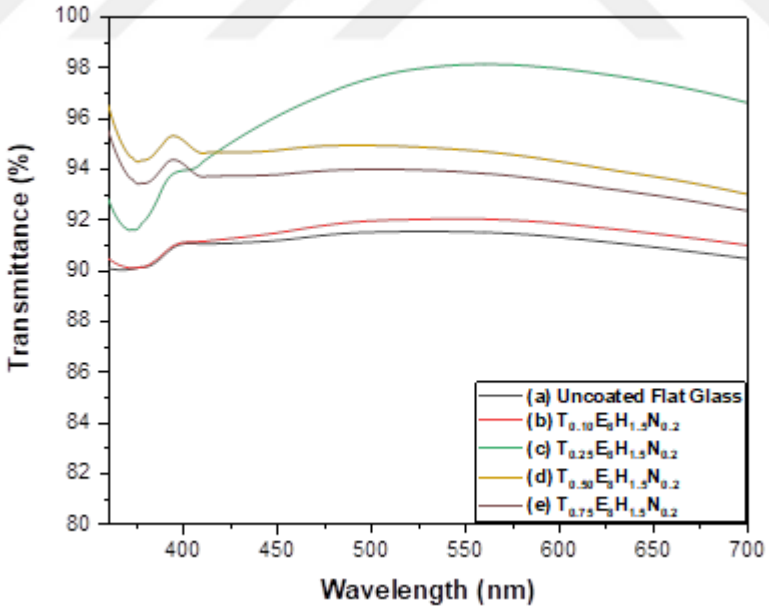


Figure 4.3 Transmittance spectra of a) uncoated glass and coatings made by using different TEOS molar ratios b) 0.1, c) 0.25, d) 0.5, e) 0.75 (T: TEOS, E: Ethanol, H: Water, N: Ammonia)

As can be seen from Figure 4.3, all anti-reflective thin film coated samples showed higher transmittance values compared to uncoated glass. Increasing the TEOS ratio from 0.10 to 0.25 in the solution increased the average visible transmittance from 92% to 98.1%. However, further increase in TEOS ratio decreased the transmittance values down to 94.7% for 0.50 molar ratio, and 93.9% for 0.75 molar ratio. This behavior is probably due to the rapid agglomeration of SiO_2 in the presence of higher TEOS ratios. As a result of this agglomeration, the porosity decreases, and hence the transmittance decreases due to light absorption in the visible range [113], [114]. As a consequence of TEOS studies, the optimum TEOS ratio was selected as 0.25 for further experimental studies.

Thirdly, in order to observe the effect of ammonia on optical performance of anti-reflective thin film coatings, the molar ratio of ammonia solution was adjusted by keeping the amount of remaining ingredients constant. It was already reported in the literature that pH control is quite important during the preparation of the solution in anti-reflective coatings since the gelation time is long when the pH value of the solution is low [115]. Therefore, in this study different solutions were prepared by using ammonia solution in the molar ratios of 0.05, 0.10, 0.15, and 0.20 and related pH values were measured (see Table 4.1). It was observed from Table 4.1 that the pH values of solutions showed an increase with increasing ammonia amount in the solution.

Table 4.1 pH values of coated samples with respect to varying ammonia molar ratio

Sample Name	$\mathbf{T_{0.25}E_8H_{1.5}N_{0.05}}$	$\mathbf{T_{0.25}E_8H_{1.5}N_{0.1}}$	$\mathbf{T_{0.25}E_8H_{1.5}N_{0.15}}$	$\mathbf{T_{0.25}E_8H_{1.5}N_{0.2}}$
pH	9.98	10.24	10.32	10.75

The visible transmittance spectra of coatings applied on flat glass substrates having different ammonia ratios are shown and compared with uncoated glass substrate in Figure 4.4.

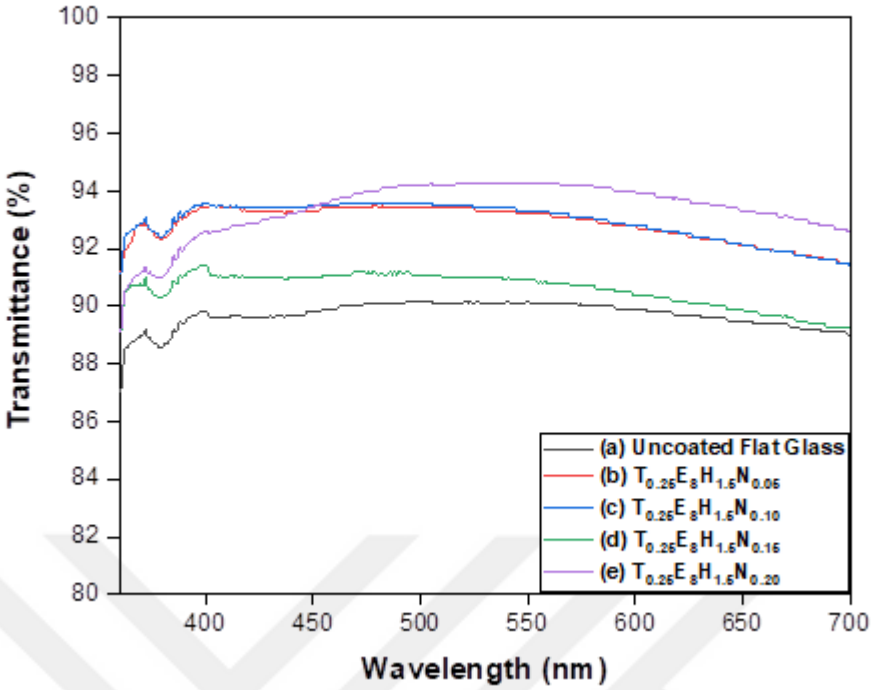


Figure 4.4 The optimum ammonia ratio was determined by checking the optical transmittance value of glasses and also by evaluating its effect on gelation time. a) uncoated b) 0.05, c) 0.10, d)0.15, e) 0.20 (T: TEOS, E: Ethanol, H: Water, N: Ammonia)

As can be seen from Figure 4.4, all anti-reflective thin film coated samples increased the transmittance to a certain extent compared to uncoated glass. The smallest increase was observed for 0.15 molar ratio, while the highest increase was observed for 0.20 molar ratio. Therefore, the optimum molar ratio was determined as 0.20.

After selecting the optimum TEOS and ammonia amounts, the starting material ratios were kept constant as TEOS:EtOH:H_2O:NH_4OH = 0.25:8:1.5:0.20 in further studies, and the effect of aging on optical performance of anti-reflective thin film coatings was studied. Aging times were initially chosen based on literature studies of Sun, Bautista, and Xiaoying [116]–[118] Therefore, three different aging periods were tested as 1, 3, 7, and 10 days. The visible transmittance spectra of coatings applied on flat glass substrates after different aging periods are depicted and compared with uncoated glass substrate in Figure 4.5.

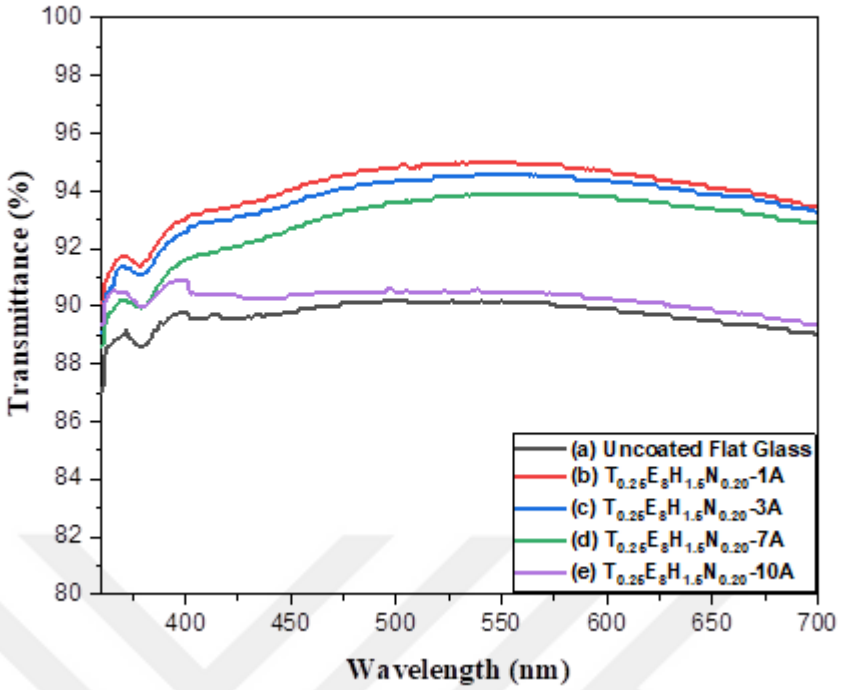


Figure 4.5 Transmittance spectra of a) uncoated glass and coatings made after different aging periods b) 1 days, c) 3 days, d) 7 days, e) 10 days (T: TEOS, E: Ethanol, H: Water, N: Ammonia, A: Aging Time)

As can be seen from Figure 4.5, all anti-reflective thin film coated samples after different aging periods increased the transmittance values compared to uncoated glass. However, the highest transmittance values were obtained for 1-day and 3-days aging as 94.3% and 95%, respectively. No significant difference was observed between 1 and 3 days of aging. Further increase in aging time decreased the transmittance values. Similar to the behavior observed in TEOS optimization studies, with increasing aging time it is reported that porosity decreases, as agglomeration increases [113], [114]. This causes a decrease in the transmission value of the thin film in the visible region. Therefore, further studies were planned to be carried out by applying both 1-day and 3-days aging as they show very close transmittance values.

Finally, to examine the effect of coating side on optical performance, single-sided (front) and double-sided (front and back) coatings were applied on flat glass substrates and aged for 1-day and 3 days. Transmittance spectra of such coatings

are shown in Figure 4.6. As also reported in the literature coating side is quite crucial in terms of transmittance of thin film coatings [119].

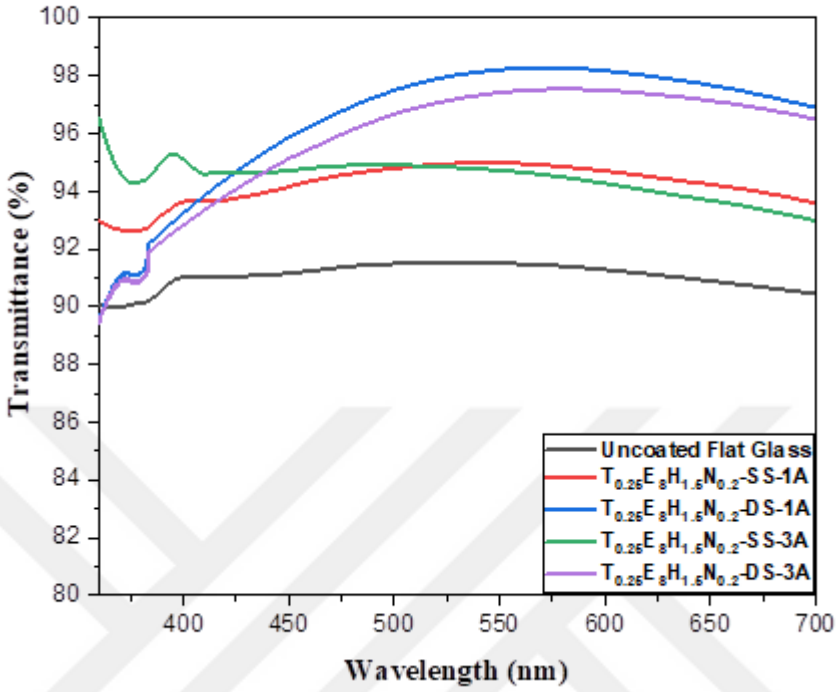


Figure 4.6 Transmittance spectra of uncoated glass along with single-sided (SS) and double-sided (DS) coatings after 1-day and 3-days aging (T: TEOS, E: Ethanol, H: Water, N: Ammonia, A: Aging Time)

As can be seen from Figure 4.6, after different aging periods one-sided and double-sided coatings increased the transmittance of uncoated substrate glasses approximately 5% and 8%, respectively. Considering the results, it was seen that the transmission values were higher in double-sided coatings. However, since both aging periods gave good transmittance values further studies were conducted by applying both 1- and 3-days aging.

In line with this information, necessary optimizations have been completed on adjusting the pH of the solution, ratio of materials used (TEOS and ammonia) in the composition, aging time, and coating-side. As a result of these optimizations, the solution preparation was repeated according to the optimum parameters and further characterizations were made using $T_{0.25}E_8H_{1.5}N_{0.2}$-SS-1A and $T_{0.25}E_8H_{1.5}N_{0.2}$-DS-1A.

Surface images are collected using scanning electron microscopy technique to check the homogeneity of coatings on the glass surface (see Figure 4.7). The coating transition line is clearly seen from the SEM image and it reveals the homogeneity of anti-reflective thin film coating on the surface.

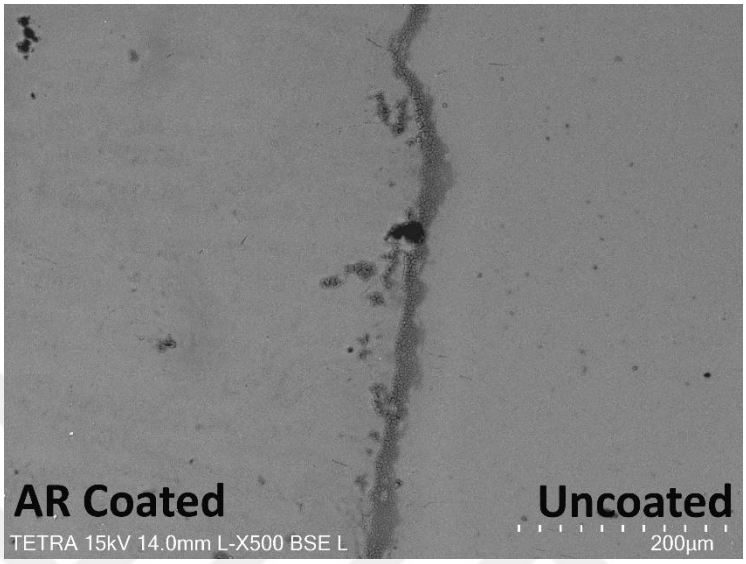


Figure 4.7 SEM image of anti-reflective thin film coated flat glass surface under 500x magnification

In order to determine the coating thickness, SEM images were also taken from the cross-section of the sample (see Figure 4.8). Therefore, prior to SEM investigations, glasses were first cut from the coating-side with a diamond cutter, and then mounted in bakelite. It was determined that the coating thickness value lies between 675 nm and 700 nm.

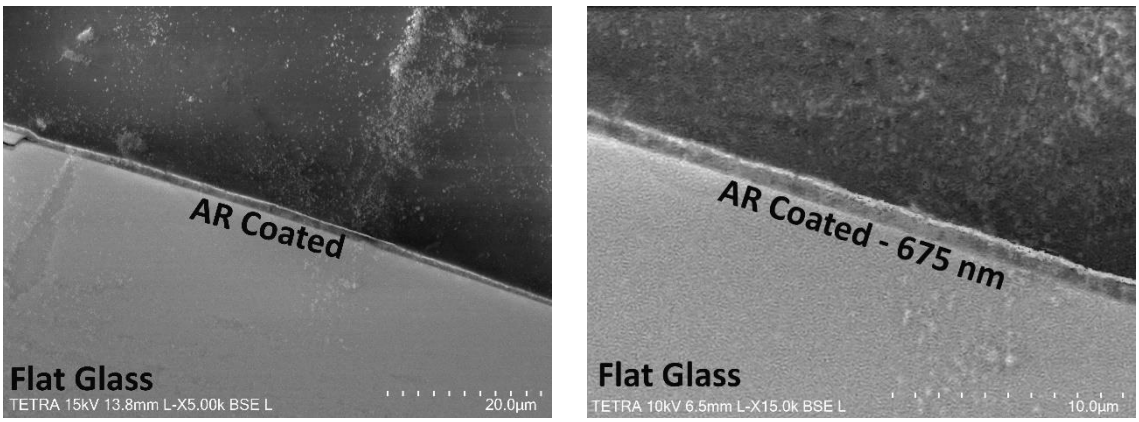


Figure 4.8 Cross-sectional SEM image of anti-reflective thin film coated flat glass revealing the coating thickness

XRD analysis was performed to check the crystallinity of thin film coatings. As shown in Figure 4.9, XRD result of anti-reflective thin film coated flat glass reveals its amorphous nature.

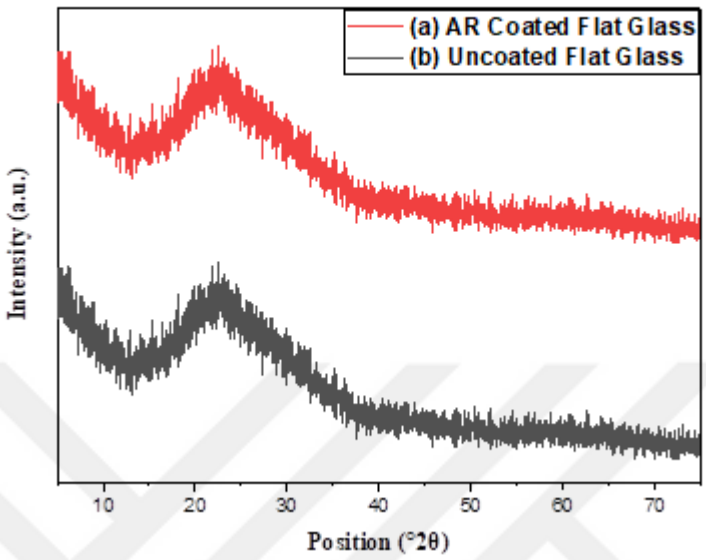


Figure 4.9 XRD result of anti-reflective thin film coated flat glass (a) and uncoated flat glass (b)

AFM analysis was performed to investigate the topography of thin film coatings (see Figure 4.10). According to the results, the average maximum height of the roughness value was found to vary between 50 and 60 nm**.**

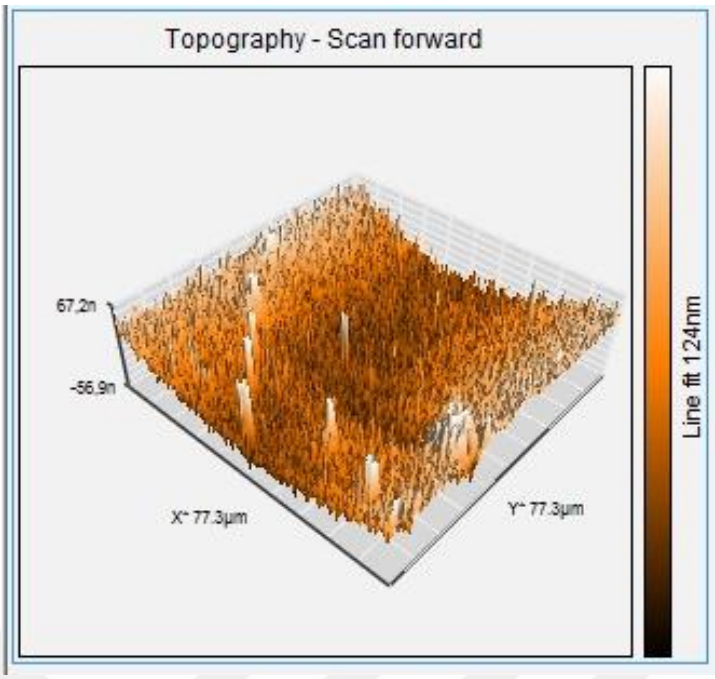


Figure 4.10 3D AFM topography image of anti-reflective thin film coated flat glass

AFM measurement was also repeated in line scan mode on the same sample (see Figure 4.11). As can be clearly seen, the average roughness value was observed as 10 nm.

Considering the obtained roughness values, as a result of dip coating of anti-reflective thin films it was understood that there was no accumulation on the sample surface except for some certain areas. In other words, a homogeneous coating was obtained.

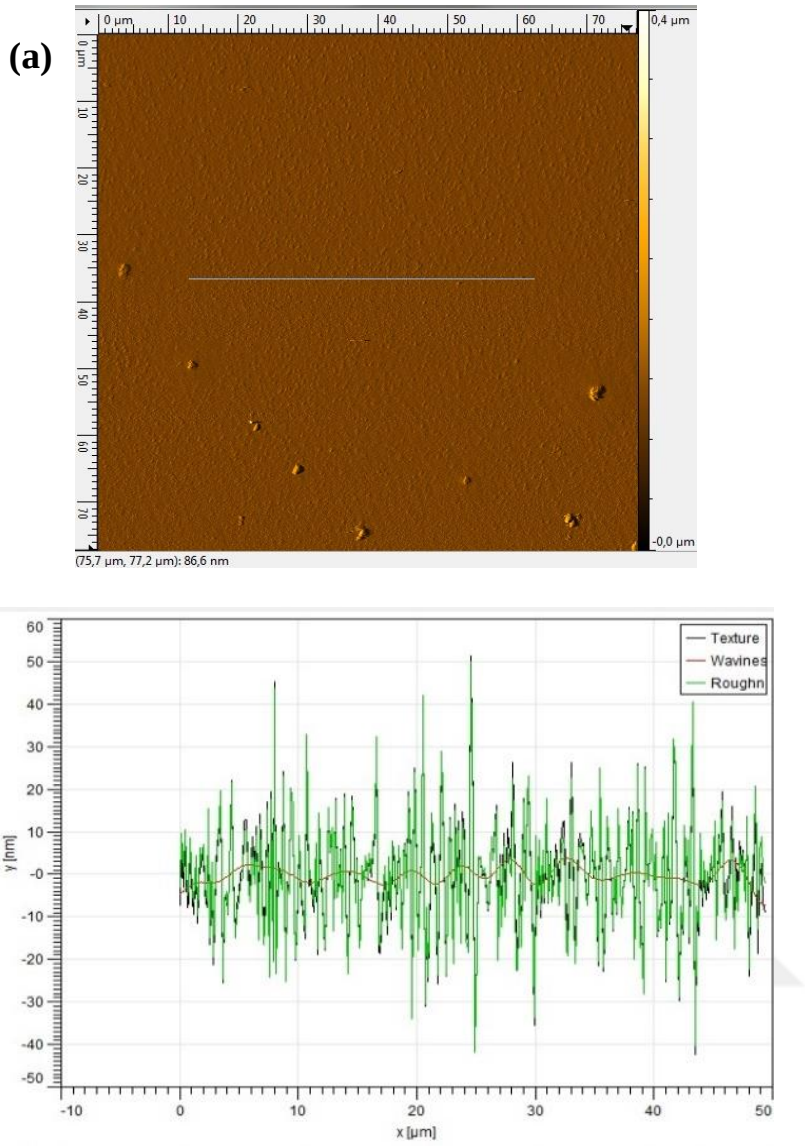


Figure 4.11 (a) 2D AFM image of anti-reflective thin film coated flat glass, and (b) variation of roughness along the selected line

XPS analysis was carried out to determine the elemental composition of anti-reflective thin film coating on flat glass surface and the results are given in Table 4.2.

Table 4.2 Elemental analysis (wt%) of anti-reflective thin film coating on flat glass surface

Si2p	O1s	Ca2p	Na1s	Mg1s	Others
36.31	37.64	0.68	0.68	0.25	5.22

In addition, a depth profile etching of 2200 seconds was applied to confirm the thickness of coating already determined by cross-sectional SEM analysis. During this

measurement time, atomic % of elements at different time periods were collected (see Figure 4.12).

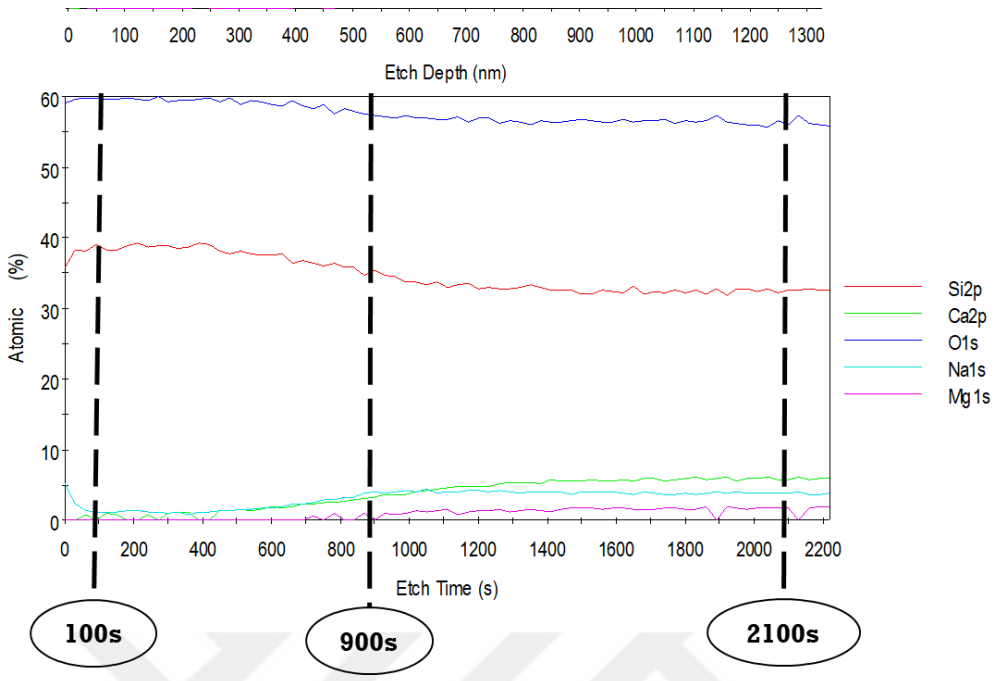


Figure 4.12 Variation of atomic % of elements with etching time

The results of atomic percentages at 100th, 900th, and 2100th seconds were analyzed to determine the point of transition from coating to the substrate and are listed in Table 4.3.

Table 4.3 Depth profile etching results for different time periods

	100 s	**900 s**	**2100 s**
Si2p	39.0782	35.4577	32.5826
Ca2p	0	3.30647	5.76935
O1s	59.8281	57.3072	56.0775
Na1s	1.09376	3.92865	3.86963
Mg1s	0	0	1.70099

Evaluating the data at 100th second, it is seen that the analysis is still on the coating surface, and no data is obtained from the elements in the glass composition. Data are only taken from Si, O, and Na. These elements originate from the coating material. Na, on the other hand, is thought to come from the pollution on the surface. As the analysis time progressed, it was observed that at the 900th second, results began to come from the glass composition, but still no information about all the elements in the glass composition. Therefore, the 900th second was determined as

the transition point from coating to glass. At the 2100th second, it was determined that information was received entirely from the composition of the glass material. Consequently, it was determined that the coating thickness is around 500-600 nm. This result confirms the value obtained in SEM analysis.

4.1.3 Anti-reflective Coatings Deposited on Prizma Patterned Glass Substrates

After optimizing sol-gel parameters on flat glasses, anti-reflective coatings were deposited on patterned glasses. When the literature is reviewed, it is seen that no similar work has been done on patterned glasses regarding the investigation of anti-reflective properties. For prizma patterned glass substrates, single-sided coatings resulted a decrease in transmittance values, therefore all coatings were applied as double-sided coatings. It is thought that such a result is due to excessive accumulation in certain areas due to the unilateral patterns on the glass surface. The visible transmittance spectra of coatings applied on prizma patterned glass substrates with different thickness values (3.2-mm and 4-mm) after different aging periods (1 day and 3 days) are shown and compared with uncoated glass substrates in Figure 4.13. It can be clearly seen that the transmittance values of uncoated 3.2-mm and 4-mm patterned glasses are 91.1% and 90%, respectively. Anti-reflective coatings aged for 1 and 3 days on 3.2 mm glass substrates increased the transmittance values up to 93.5% and 97%, respectively. For coatings applied on 4 mm glass substrates the transmittance values showed an increase to 93.5% and 96.5% for 1-day and 3-days aging, respectively. As expected, it can be concluded that the transmittance values decrease with increasing thickness and aging time.

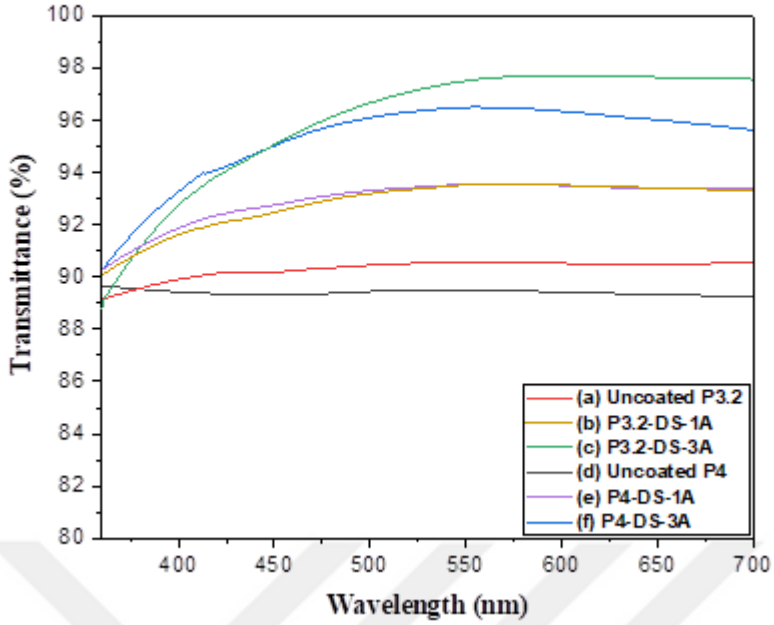


Figure 4.13 Transmittance spectra of prizma glasses and coatings made after different aging periods a) uncoated-3.2 mm, b) 3.2 mm-double sided-1 day, c) 3.2 mm-double sided-3 days, d) uncoated-4 mm, e) 4 mm-double sided-1 day, f) 4 mm-double sided-3 days (P: Prizma, DS: Double-Sided, A: Aging Time)

Surface images are collected using optical microscopy to check the homogeneity of coatings on the glass surface. Optical microscope image of anti-reflective thin film coated prizma patterned glass surface is shown in Figure 4.14.

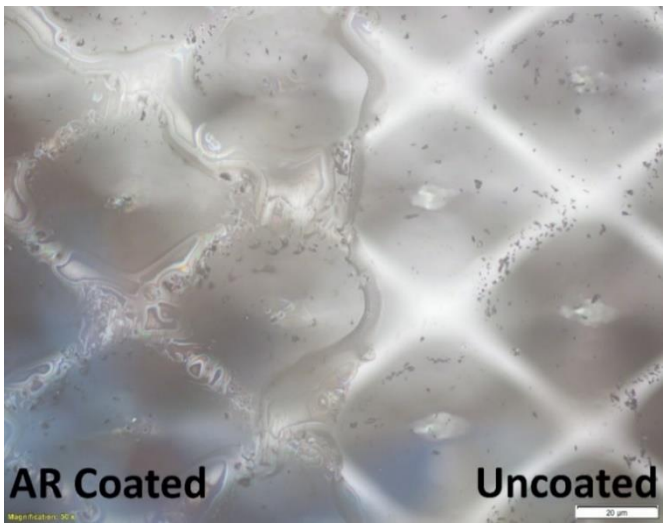


Figure 4.14 Optical microscope image of anti-reflective thin film coated prizma patterned glass surface under 50X magnification

SEM image of anti-reflective thin film coated prizma patterned glass surface is given in Figure 4.15 for a more detailed investigation of the coating surface. It is clearly seen from the image that the coating is not homogeneous, and the solution accumulates at the bottom of the pyramid patterns.

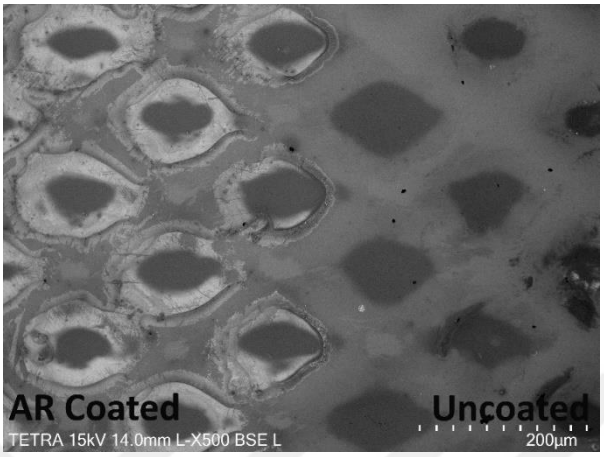


Figure 4.15 SEM image of anti-reflective thin film coated prizma patterned glass surface under 500x magnification

Afterwards, XRD analysis was performed to check the phase characteristics of thin film coatings. As shown in Figure 4.16, XRD analysis of anti-reflective thin film coated prizma patterned glass reveals the amorphous nature of coating.

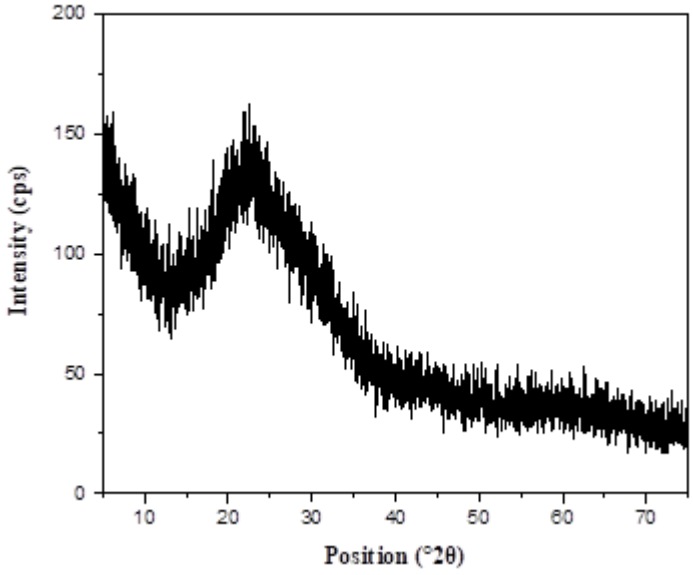


Figure 4.16 XRD result of anti-reflective thin film coated prizma patterned glass

4.1.4 Anti-reflective Coatings Deposited on Sandy Patterned Glass Substrates

Similar to prizma patterned glasses, for sandy patterned glass substrates single-sided coatings resulted a decrease in transmittance values, therefore all coatings were applied as double-sided coatings. The visible transmittance spectra of coatings applied on sandy patterned glass substrates with different thickness values (3.2-mm and 4-mm) after different aging periods (1 day and 3 days) are shown and compared with uncoated glass substrates in Figure 4.17. It can be clearly seen that the transmittance values of uncoated 3.2-mm and 4-mm patterned glasses are 91.3% and 90.1%, respectively. Anti-reflective coatings aged for 1 and 3 days on 3.2 mm glass substrates increased the transmittance values up to 95.5% and 99.1%, respectively. For coatings applied on 4 mm glass substrates the transmittance values showed an increase to 92% and 97.6% for 1-day and 3-days aging, respectively. As expected, it can be concluded that the transmittance values decrease with increasing thickness and aging time.

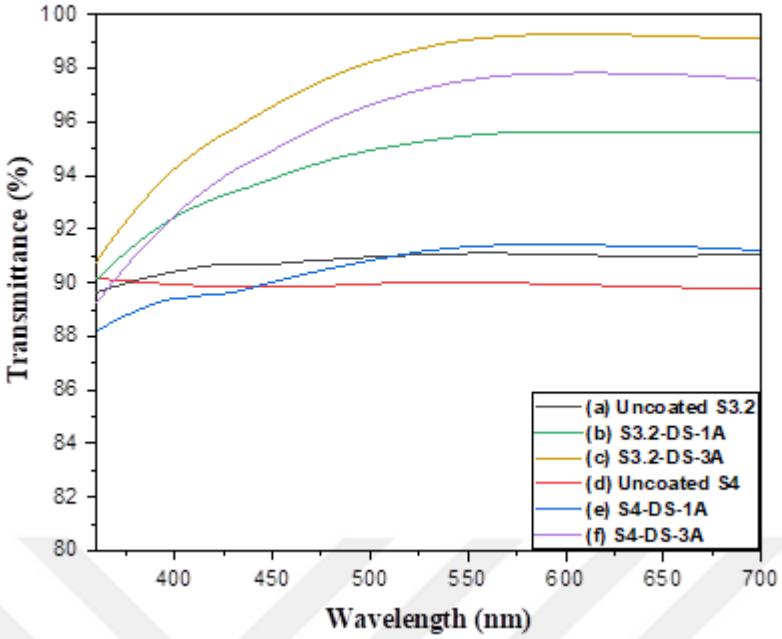


Figure 4.17 Transmittance spectra of sandy glasses and coatings made after different aging periods a) uncoated-3.2 mm, b) 3.2 mm-double sided-1 day, c) 3.2 mm-double sided-3 days, d) uncoated-4 mm e) 4 mm-double sided-1 day, f) 4 mm-double sided-3 days (S: Sandy, DS: Double-Sided, A: Aging Time)

Surface images are collected using optical microscopy to check the homogeneity of coatings on the glass surface. Optical microscope image of anti-reflective thin film coated sandy patterned glass surface is shown in Figure 4.18. Surface morphology was examined by selecting 3 different points from the sample surface. The transition points are clearly visible from optical images. It can be inferred that the coating adheres to sandy patterned glasses.

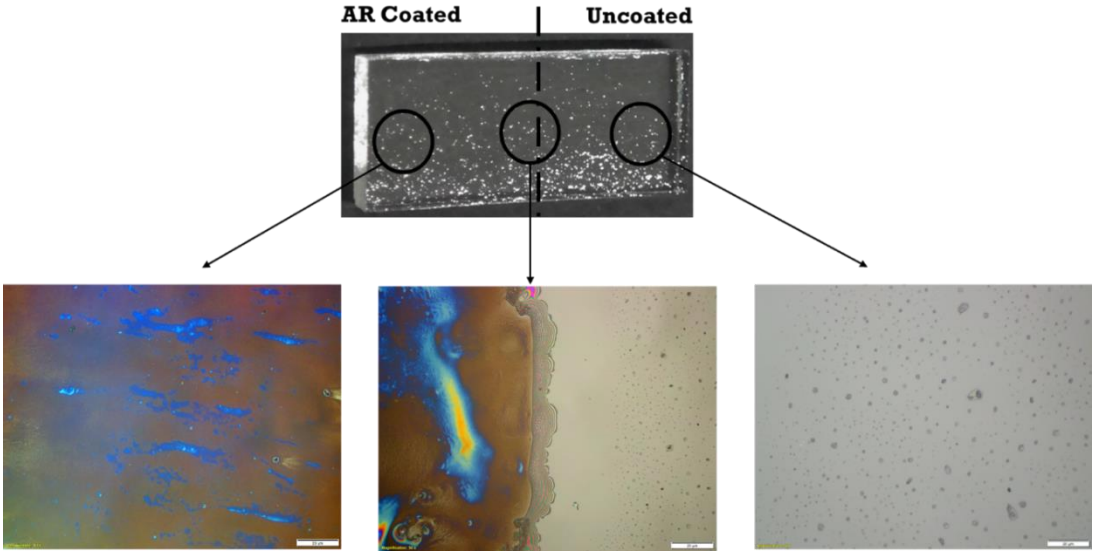


Figure 4.18 Optical microscope images of anti-reflective thin film coated sandy patterned glass surface under 50X magnification

SEM image of anti-reflective thin film coated sandy patterned glass surface is given in Figure 4.19 for a more detailed investigation of the coating surface. It is clearly seen from the image that the coating is homogeneous, and no accumulation occurs in sandy patterned glasses. Since sandy patterned glasses have a more homogeneous coating, they show higher transmittance values compared to prizma patterned glasses.

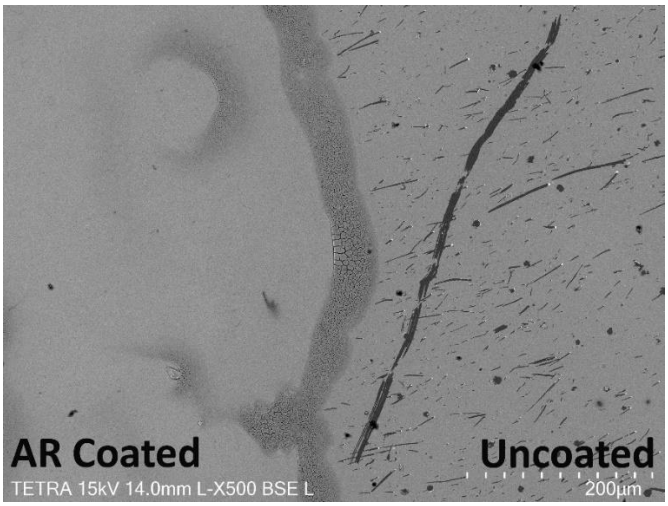


Figure 4.19 SEM image of anti-reflective thin film coated sandy patterned glass surface under 500x magnification

Finally, XRD analysis was carried out to see whether the coating is amorphous or crystalline in sandy patterned glasses. The analysis result is given in Figure 4.20. As

can be understood from the XRD results, it was determined that the coatings in these samples were also amorphous.

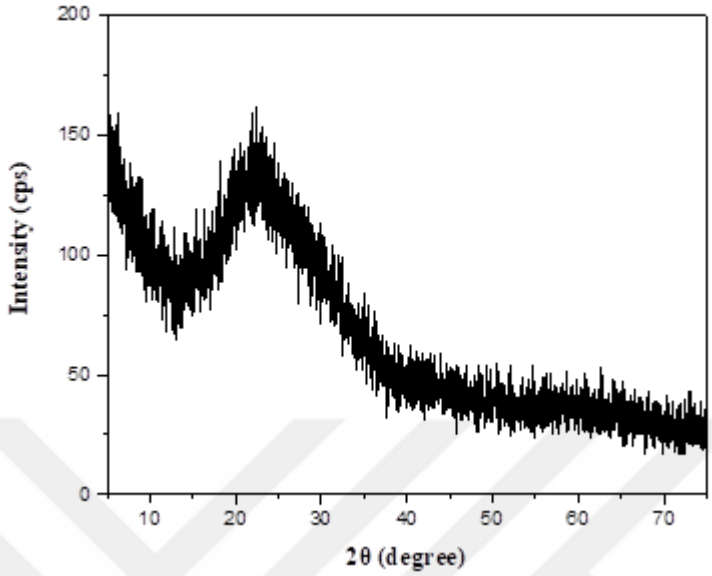


Figure 4.20 XRD result of anti-reflective thin film coated sandy patterned glass

4.1.5 Comparison of Anti-reflective Coatings on Different Glass Substrates

As a result of optimization studies using 1.1 mm thick flat soda-lime silicate glass substrates, the optimum molar ratio of the anti-reflective solution was determined as follows: TEOS:EtOH:H_2O:NH_4OH = 0.25:8:1.5:0.2. Considering the gelation time, it was determined that the ideal pH value should be between 9-10. Then, the coatings were deposited on prizma and sandy glasses to investigate the effect of anti-reflective coatings on patterned glasses. The transmittance values were measured using solutions aged at different durations. While there is no significant difference in 1- and 3-days aging periods in flat glasses, higher transmission values were obtained after 3 days of aging in patterned glasses. In addition, higher visible light transmittance was obtained in double-sided coatings in all glass types. From Table 4.4, it can be seen that transmittance values of flat, prizma, and sandy patterned glasses increase up to 98%, 97%, and 99%, respectively. To conclude, the maximum visible light transmittance value is obtained in sandy patterned glasses among all glass types.

Table 4.4 Transmittance values of uncoated glasses along with double-sided (DS) coatings after 1-day and 3-days aging (T: TEOS, E: Ethanol, H: Water, N: Ammonia, A: Aging Time, S: Sandy, P: Prizma)

Glass Types	Sample Code	Transmittance (%)	
		Uncoated	AR Coated
Flat Glass	$T_{0.25}E_8H_{1.5}N_{0.2}$-DS-1A	90.5	98.1
	$T_{0.25}E_8H_{1.5}N_{0.2}$-DS-3A		97.2
Prizma Glass	P3.2-DS-1A	91.1	93.5
	P3.2-DS-3A		97
	P4-DS-1A	90	93.5
	P4-DS-3A		96.5
Sandy Glass	S3.2-DS-1A	91.3	95.5
	S3.2-DS-3A		99.1
	S4-DS-1A	90.1	92
	S4-DS-3A		97.6

4.2 Conclusions and Recommendations

The crucial findings of this dissertation study can be summarized as follows:

1. According to the optimization of gelation time studies, it was observed that while the gelation time for the acidic solution prepared with HCl (pH= 3) varied between 7-10 days, the gelation time varied between 1-3 days for the basic solution prepared with NH_4OH (pH= 10). Therefore, it was concluded that the gelation time decreased as the solution pH increased.
2. According to the optimization of TEOS amount in the solution, it was observed that increasing the TEOS ratio in the solution results in rapid agglomeration of SiO_2. As a result of this agglomeration, it is thought that the porosity decreases, and hence the transmittance decreases due to light absorption in the visible range. Therefore, the highest visible light transmittance value (98.1%) was obtained for low TEOS ratios i.e., the solution where 0.25 molar TEOS ratio was used.
3. As a result of studies on different amount of ammonia containing solutions, it was observed that the pH value increased with increasing ammonia amount. It was observed that the polymerization in the solution increased and the gelation time decreased with the increase in pH. The best gelling was

achieved especially when pH is 10. This pH value was obtained when 0.20 molar ammonia solution was used in the solution.

4. The gelation of the solution depends not only on the pH value but also on the aging time. Therefore, solutions were subjected to different aging periods as 1, 3, 7, 10 days. As a result, it was observed that visible light transmittance decreases with increasing aging time.
5. For the examination of the effect of coating side on optical performance, single-sided and double-sided coatings were applied on glass substrates and it was observed that visible transmission values were higher in double-sided coatings.
6. As a result of the coatings made on 3.2 mm thick prizma patterned glasses, a visible light transmittance of 93.5% after 1 day aging and 97% after 3 days of aging was obtained. In 4 mm thick prizma patterned glasses, visible light transmittance was obtained as 93.5% after 1 day aging, and 96.5% after 3 days aging. Therefore, the highest transmittance value was achieved with the coatings obtained after 3 days of aging in 3.2 mm thick prizma patterned glasses as 97%.
7. As a result of the coatings made on 3.2 mm thick sandy patterned glasses, a visible light transmittance of 95.5% after 1 day aging and 99.1% after 3 days of aging was obtained. In 4 mm thick sandy patterned glasses, visible light transmittance was obtained as 92% after 1 day aging, and 97.6% after 3 days aging. Therefore, the highest transmittance value was achieved with the coatings obtained after 3 days of aging in 3.2 mm thick sandy patterned glasses as 99.1%.
8. The anti-reflective coatings on glass substrates were found to be amorphous according to the XRD results. As a result of XPS analysis, it was determined that only Si and O elements exist in the coating.
9. Optical microscopy and SEM investigations revealed that the coatings were homogeneous on glass substrates.
10. Finally, for anti-reflective film coated 3.2 mm prizma and sandy patterned glasses visible transmittance values were found to be around 97% and 99%, respectively. This reveals that anti-reflective film coated patterned glasses

have a great potential to be used as cover glasses to increase the overall efficiency of PV systems. Considering the experimental findings, application of anti-reflective coatings to thinner patterned glasses have the possibility to further increase the visible light transmission, thus enhancing the efficiency of photovoltaic systems. Therefore, it is recommended that similar studies should be conducted on thinner patterned glasses in the future. Furthermore, mechanical strength of glasses used in photovoltaic systems is also of great importance. For this reason, in future works, the effect of anti-reflective coatings on chemically-strengthened thin patterned glasses should also be studied.

REFERENCES

[1] D. M. Fischer, "International Technology Roadmap for Photovoltaic (ITRPV) - Results 2017," *Itrpv*, vol. 9. 2018.

[2] N. L. Panwar, S. C. Kaushik, and S. Kothari, "Role of renewable energy sources in environmental protection: A review," *Renewable and Sustainable Energy Reviews*, vol. 15, no. 3. pp. 1513–1524, 2011.

[3] J. Deubener, G. Helsch, A. Moiseev, and H. Bornhöft, "Glasses for solar energy conversion systems," *J. Eur. Ceram. Soc.*, vol. 29, no. 7, pp. 1203–1210, 2009.

[4] C. H. Yeh, F. Y. Chang, H. T. Young, T. Y. Hsieh, and C. H. Chang, "Transparent solar concentrator for flat panel display," *Jpn. J. Appl. Phys.*, vol. 51, no. 6 PART 2, 2012.

[5] A. Luque and S. Hegedus, *Handbook of Photovoltaic Science and Engineering*. 2011.

[6] D. J. C. Mackay, *Sustain. Energy — without hot air. Cambridge, UK UIT Cambridge Ltd*, 2009.

[7] B. M. Freiburger, K. Isbilir, F. Lisco, G. Womack, J. M. Walls, and C. S. Thompson, "Durable High-performance Water-based Anti-Reflective Coating for PV Module Glass," *2018 IEEE 7th World Conf. Photovolt. Energy Conversion, WCPEC 2018 - A Jt. Conf. 45th IEEE PVSC, 28th PVSEC 34th EU PVSEC*, pp. 2126–2128, 2018.

[8] F. Giovannetti, S. Föste, N. Ehrmann, and G. Rockendorf, "High transmittance, low emissivity glass covers for flat plate collectors: Applications and performance," *Energy Procedia*, vol. 30, pp. 106–115, 2012.

[9] S. B. Khan, H. Wu, and Z. Zhang, "Omnidirectional SiO_2 AR coatings," *Coatings*, vol. 8, no. 6, 2018.

[10] C. S. Solanki and H. K. Singh, *Anti-reflection and Light Trapping in c-Si Solar Cells*, no. Tanaka 2010. 2017.

[11] C. R. Kurkjian and W. R. Prindle, "Perspectives on the history of glass

composition," *J. Am. Ceram. Soc.*, vol. 81, no. 4, pp. 795–813, 1998.

[12] R. Prado, G. Beobide, A. Marcaide, J. Goikoetxea, and A. Aranzabe, "Development of multifunctional sol-gel coatings: Anti-reflection coatings with enhanced self-cleaning capacity," *Sol. Energy Mater. Sol. Cells*, vol. 94, no. 6, pp. 1081–1088, 2010.

[13] G. Helsch and J. Deubener, "Interface crystallization of ceria in porous silica films for solar applications," *Crystals*, vol. 7, no. 3, 2017.

[14] C. Agustín-Sáenz, M. Machado, and A. Tercjak, "Antireflective mesoporous silica coatings by optimization of water content in acid-catalyzed sol-gel method for application in glass covers of concentrated photovoltaic modules," *J. Colloid Interface Sci.*, vol. 534, pp. 370–380, 2019.

[15] J. Dziedzic and M. Inglot, "Ultrathin glass for the photovoltaic applications," *Acta Physica Polonica A*, vol. 132, no. 1. pp. 176–178, 2017.

[16] E. R. Brinley, "Tunable Nanostructure Anti-Reflective Coatings" p. 45, 2007.

[17] S. D. Wang and Y. Y. Shu, "Superhydrophobic antireflective coating with high transmittance," *J. Coatings Technol. Res.*, vol. 10, no. 4, pp. 527–535, 2013.

[18] L. Tang *et al.*, "Large-scale, adhesive-free and omnidirectional 3D nanocone anti-reflection films for high performance photovoltaics," *J. Semicond.*, vol. 40, no. 4, 2019.

[19] M. Kim *et al.*, "Antireflective, self-cleaning and protective film by continuous sputtering of a plasma polymer on inorganic multilayer for perovskite solar cells application," *Sol. Energy Mater. Sol. Cells*, vol. 191, no. November 2018, pp. 55–61, 2019.

[20] Y. Hashimoto and T. Yamamoto, "Fabrication of an anti-reflective and super-hydrophobic structure by vacuum ultraviolet light-assisted bonding and nanoscale pattern transfer," *Micromachines*, vol. 9, no. 4, 2018.

[21] S. Islam, R. A. Rahman, S. Riaz, S. Naseem, Z. Ottoman, and M. A. Saeed, "*Study of Sol-gel Based Antireflection Coatings*," vol. 2, no. 10. Elsevier Ltd., 2015.

[22] N. EKREN, "Researches on Anti-reflection Coating (ARC) Methods Used in PV

Systems," *Balk. J. Electr. Comput. Eng.*, vol. 6, no. 1, pp. 42–46, 2018.

[23] L. Ye, S. Zhang, Q. Wang, L. Yan, H. Lv, and B. Jiang, "Mechanically stable single-layer mesoporous silica antireflective coating on solar glass," *RSC Adv.*, vol. 4, no. 67, pp. 35818–35822, 2014.

[24] N. Shanmugam, R. Pugazhendhi, R. M. Elavarasan, P. Kasiviswanathan, and N. Das, "Anti-reflective coating materials: A holistic review from PV perspective," *Energies*, vol. 13, no. 10, pp. 1–93, 2020.

[25] G. Vani Padmaja, "Preparation of Orthosilicic Acid by Sol-Gel Technique using Tetraethyl orthosilicic acid (TEOS) and its applications.," *Int. J. Sci. Res. Publ.*, vol. 5, no. 1, pp. 2250–3153, 2014.

[26] G. E. L. Processing, "Handbook of sol-gel science and technology: processing, characterization, and applications," *Choice Rev. Online*, vol. 42, no. 10, pp. 42-5885-42–5885, 2005.

[27] T. Coan, G. S. Barroso, G. Motz, A. Bolzána, and R. A. F. Machado, "Preparation of PMMA/hBN composite coatings for metal surface protection," *Mater. Res.*, vol. 16, no. 6, pp. 1366–1372, 2013.

[28] S. Amiri and A. Rahimi, "Hybrid nanocomposite coating by sol–gel method: a review," *Iran. Polym. J. (English Ed.*, vol. 25, no. 6, pp. 559–577, 2016.

[29] A. Kumar, N. Yadav, M. Bhatt, N. K. Mishra, P. Chaudhary, and R. Singh, "Sol-gel method," *Oyobuturi*, vol. 62, no. 12, pp. 1248–1249, 1993.

[30] U. Pantulap, B. Petchareanmongkol, W. Kaewdang, and K. Tapasa, "Optical transparent and hydrophobic properties of TEOS/OTES hybrid materials by sol-gel processing," *Key Eng. Mater.*, vol. 798 KEM, pp. 134–139, 2019.

[31] Y. Belce and F. Cebeci, "Multilayer thin films of Zinc (II) Phthalocyanine loaded Poly(D, L-lactide-co-glycolide) nanocapsules by layer-by-layer self assembly," *Mater. Res. Express*, vol. 6, no. 7, 2019.

[32] Y. H. Huang, L. C. Chen, and H. M. Chou, "Optimization of process parameters for anti-glare spray coating by pressure-feed type automatic air spray gun using response surface methodology," *Materials (Basel).*, vol. 12, no. 5, 2019.

[33] M. S. Mozumder, A. H. I. Mourad, H. Pervez, and R. Surkatti, “Recent developments in multifunctional coatings for solar panel applications: A review,” *Sol. Energy Mater. Sol. Cells*, vol. 189, no. September 2018, pp. 75–102, 2019.

[34] A. Qazi *et al.*, “Towards Sustainable Energy: A Systematic Review of Renewable Energy Sources, Technologies, and Public Opinions,” *IEEE Access*, vol. 7. pp. 63837–63851, 2019.

[35] Z. Han, X. Feng, Z. Guo, S. Niu, and L. Ren, “Flourishing Bioinspired Antifogging Materials with Superwettability: Progresses and Challenges,” *Adv. Mater.*, vol. 30, no. 13, pp. 1–32, 2018.

[36] N. Tsoy, V. Prado, A. Wypkema, J. Quist, and M. Mourad, “Anticipatory Life Cycle Assessment of sol-gel derived anti-reflective coating for greenhouse glass,” *J. Clean. Prod.*, vol. 221, pp. 365–376, 2019.

[37] IRENA, “Renewable Energy Statistics 2019,” *International Renewable Energy Agency*, vol. 1, no. 1. p. 348, 2019.

[38] S. G. Azevedo, M. Santos, and J. R. Antón, “Supply chain of renewable energy: A bibliometric review approach,” *Biomass and Bioenergy*, vol. 126. pp. 70–83, 2019.

[39] H. W. S. A. Goetzberger, C. Hebling, “Photovoltaic Materials: History, Status and Outlook Material,” *Sci. Eng. R*, vol. 16803, no. 40.

[40] M.A. Green, “Third Generation Photovoltaics: Advanced Solar Energy Conversion,” *Springer Berlin, Ger.*, 2003.

[41] (IEA) International Energy Agency, “Assessment of PV Module Failures in the Field,” *IEA-Photovoltaic Power Systems Programme*. 2017.

[42] P. R. M. Eckhart, M. El-Ashry, D. Hales, K. Hamilton, “Renewables 2018 Global Status Report,” no. p.33, 2020.

[43] N. Ozer, "*Sol-Gel Optics: Processing and applications*," vol. 43, no. 3. 1996.

[44] S. Luo, Q.; Deng, X.; Zhang, C.; Yu, M.; Zhou, X.; Wang, Z.; Chen, X.; Huang, “Enhancing photovoltaic performance of perovskite solar cells with silica

nanosphere antireflection coatings," *Sol. Energy*, vol. 128–135, p. 16, 2018.

[45] V. R. G. Rajan, K. Aryal, T. Ashrafee, S. Karki, S. Babcock, "Realtime Optimization of Anti-reflective Coating for CIGS Solar Cells, Photovoltaic Specialists Conference (PVSC)," *IEEE*, vol. 2250–2253, no. 43rd, 2016.

[46] H. L. D. Huh, J. Shin, M. Byun, S. Son, P. Jung, H. Choi, Y. Kim, "Analysis of long-term monitoring data of PV modüle with Siox-based anti-reflective patterned protective glass," *Sol. energy Mater. Sol. cells*, vol. 170, pp. 33–38, 2017.

[47] M. D. A. and R. H. (Eds.), "Clean Electricity from Photovoltaics," *Imp. Coll. Press London, UK*, vol. Volume 1 o, 2003.

[48] W. Zhang, J. Tu, W. Long, W. Lai, Y. Sheng, and T. Guo, "Preparation of SiO_2 anti-reflection coatings by sol-gel method," *Energy Procedia*, vol. 130, pp. 72–76, 2017.

[49] M. GREEN *et al.*, "Solar cell efficiency tables," *Ieee Trans Fuzzy Syst*, vol. 20, no. 6, pp. 1114–1129, 2012.

[50] I. A. Digdaya, "Optical Enhancement for Heterojunction Silicon Solar Cells," 2012.

[51] A. Mohammad Bagher, "Types of Solar Cells and Application," *Am. J. Opt. Photonics*, vol. 3, no. 5, p. 94, 2015.

[52] R. A. Messenger, "*Photovoltaic Systems Engineering,*" 2018.

[53] B. L. Allsopp *et al.*, "Towards improved cover glasses for photovoltaic devices," *Prog. Photovoltaics Res. Appl.*, vol. 28, no. 11, pp. 1187–1206, 2020.

[54] K. Chandra Sekhar Reddy, D. Karthik, D. Bhanupriya, K. Ganesh, M. Ramakrishna, and S. Sakthivel, "Broad band antireflective coatings using novel in-situ synthesis of hollow MgF_2 nanoparticles," *Sol. Energy Mater. Sol. Cells*, vol. 176, no. December, pp. 259–265, 2018.

[55] T. Surek, "Crystal Growth and Materials Research in Photovoltaics: Progress and Challenges," *J. Cryst. Growth 275*, vol. 292–304.

[56] Y. Yuan, Y. Chen, W. L. Chen, and R. J. Hong, "Preparation, durability and

thermostability of hydrophobic antireflective coatings for solar glass covers," *Sol. Energy*, vol. 118, pp. 222–231, 2015.

[57] S. B. Khan, H. Wu, C. Pan, and Z. Zhang, "A Mini Review : Antireflective Coatings Processing Techniques , Applications and Future Perspective," vol. 5, no. 4, pp. 36–54, 2017.

[58] B. T. Liu and W. De Yeh, "Antireflective surface fabricated from colloidal silica nanoparticles," *Colloids Surfaces A Physicochem. Eng. Asp.*, vol. 356, no. 1–3, pp. 145–149, 2010.

[59] S. Jalaly, M. Vahdani, M. Shahabadi, and G. M. Mohamad Sadeghi, "Design, fabrication, and measurement of a polymer-based anti-reflection coating for improved performance of a solar panel under a specific incident angle," *Sol. Energy Mater. Sol. Cells*, vol. 189, no. September 2018, pp. 175–180, 2019.

[60] ITRPV, "International Technology Roadmap for Photovoltaics (ITRPV) 8 th edition : Crystalline Silicon Technology– Current Status and Outlook," *Workshop ITRPV – VDMA Photovoltaic Equipment*. pp. 1–40, 2017.

[61] D. Huh, H. J. Choi, M. Byun, K. Kim, and H. Lee, "Long-term analysis of PV module with large-area patterned anti-reflective film," *Renew. Energy*, vol. 135, pp. 525–528, 2019.

[62] M. Rutan, "Abrasion Resistant Anti-Reflective Sol-Gel Coatings," 2011.

[63] X. Li, X. Yu, and Y. Han, "Polymer thin films for antireflection coatings," *J. Mater. Chem. C*, vol. 1, no. 12, pp. 2266–2285, 2013.

[64] J. A. Xi, J.-Q.; Schubert, M.F.; Kim, J.K.; Schubert, E.F.; Chen, M.; Lin, S.-Y.; Liu, W.; Smart, "Optical thin-film materials with low refractive index for broadband elimination of Fresnel reflection," *Nat. Photonics*, pp. 176–179, 2007.

[65] J. Y. Y. Loh, D. P. Puzzo, P. G. O'Brien, G. A. Ozin, and N. P. Kherani, "Enhancing photovoltaics with broadband high-transparency glass using porosity-tuned multilayer silica nanoparticle anti-reflective coatings," *RSC Adv.*, vol. 4, no. 59, pp. 31188–31195, 2014.

[66] H. K. Raut, V. A. Ganesh, A. S. Nair, and S. Ramakrishna, “Anti-reflective coatings: A critical, in-depth review,” *Energy Environ. Sci.*, vol. 4, no. 10, pp. 3779–3804, 2011.

[67] D. Chen, “Anti-reflection (AR) coatings made by sol-gel processes: A review,” *Sol. Energy Mater. Sol. Cells*, vol. 68, no. 3–4, pp. 313–336, 2001.

[68] X. Zhang *et al.*, “Moth-eye-like antireflection coatings based on close-packed solid/hollow silica nanospheres,” *J. Sol-Gel Sci. Technol.*, vol. 90, no. 2, pp. 330–338, 2019.

[69] M. C. Clapham, P.B.; Hutley, “Reduction of Lens Reflexion by the ‘Moth Eye’ Principle,” *Nature*, no. 244, pp. 281–282, 1973.

[70] X. X. Zhang *et al.*, “Template-free sol-gel preparation of superhydrophobic ORMOSIL films for double-wavelength broadband antireflective coatings,” *Adv. Funct. Mater.*, vol. 23, no. 35, pp. 4361–4365, 2013.

[71] W. Li *et al.*, “Broadband antireflective and superhydrophobic coatings for solar cells,” *Mater. Today Energy*, vol. 12, pp. 348–355, 2019.

[72] J. Woo Leem, J.; Guan, X.-Y.; Choi, M.; Su Yu, “Broadband and omnidirectional highly-transparent coverglasses coated with biomimetic moth-eye nanopatterned polymer films for solar photovoltaic system applications,” *Sol. Energy Mater. Sol. Cells*, vol. 134, pp. 45–53, 2015.

[73] W. Glaubitt and P. Löbmann, “Antireflective coatings prepared by sol-gel processing: Principles and applications,” *J. Eur. Ceram. Soc.*, vol. 32, no. 11, pp. 2995–2999, 2012.

[74] M. Manca, A. Cannavale, L. De Marco, A. S. Aricò, R. Cingolani, and G. Gigli, “Durable superhydrophobic and antireflective surfaces by trimethylsilanized silica nanoparticles-based sol-gel processing,” *Langmuir*, vol. 25, no. 11, pp. 6357–6362, 2009.

[75] M. S. Zaier, A.; Meftah, A.; Jaber, A.Y.; Abdelaziz, A.A.; Aida, “Annealing effects on the structural, electrical and optical properties of ZnO thin films prepared by thermal evaporation technique,” *J. King Saud Univ. Sci.*, vol. 356–360, p. 27,

2015.

[76] U. Walheim, S.; Walheim, S.; Schaffer, E.; Mlynek, J.; Steiner, "Nanophase-Separated Polymer Films as High-Performance Antireflection Coatings," *Science (80).*, vol. 520–522, p. 283, 1999.

[77] R. A. Sopori, B.L.; Pryor, "Design of antireflection coatings for textured silicon solar cells," *Sol. Cells*, vol. 249–261, p. 8, 1983.

[78] C. Tao *et al.*, "Hydrophobic antireflective coatings with ultralow refractive index synthesized by deposition of methylated hollow silica nanoparticles," *Mater. Lett.*, vol. 183, pp. 374–377, 2016.

[79] Z. Han, Z. Jiao, S. Niu, and L. Ren, "Ascendant bioinspired antireflective materials: Opportunities and challenges coexist," *Prog. Mater. Sci.*, vol. 103, no. January, pp. 1–68, 2019.

[80] A. . Papet, P.; Nichiporuk, O.; Kaminski, A.; Rozier, Y.; Kraiem, J.; Lelievre, J.-F.; Chaumartin, A.; Fave and M. Lemiti, "Pyramidal texturing of silicon solar cell with TMAH chemical anisotropic etching," *Sol. Energy Mater. Sol. Cells*, vol. 2319–2328, no. 90, 2006.

[81] M. Remache, L.; Fourmond, E.; Mahdjoub, A.; Dupuis, J.; Lemiti, "Design of porous silicon/PECVD SiOx antireflection coatings for silicon solar cells," *Mater. Sci. Eng. B*, vol. 176, pp. 45–48, 2011.

[82] A. Behera, P. Mallick, and S. S. Mohapatra, "Nanocoatings for anticorrosion," *Corros. Prot. Nanoscale*, pp. 227–243, 2020.

[83] P. Creighton, J.R., Ho, "Introduction to Chemical Vapor Deposition (CVD)," *ASM Int.*, 2001.

[84] B. Fotovvati, N. Namdari, and A. Dehghanghadikolaei, "On coating techniques for surface protection: A review," *J. Manuf. Mater. Process.*, vol. 3, no. 1, 2019.

[85] H. G. Floch and P. F. Belleville, "Optical thin films from the sol-gel process," *Opt. Interf. Coatings*, vol. 2253, no. November 1994, p. 764, 1994.

[86] D. F. Zambrano *et al.*, "Mechanical and microstructural properties of broadband anti-reflective TiO_2/SiO_2 coatings for photovoltaic applications

fabricated by magnetron sputtering," *Sol. Energy Mater. Sol. Cells*, vol. 220, no. September 2020, 2021.

[87] G. Pinto, F. Silva, J. Porteiro, J. Míguez, and A. Baptista, "Numerical simulation applied to PVD reactors: An overview," *Coatings*, vol. 8, no. 11, pp. 1–20, 2018.

[88] H.-U. Krebs *et al.*, "Pulsed Laser Deposition (PLD) - A Versatile Thin Film Technique," no. May 2014, pp. 505–518, 2003.

[89] S. N. Ogugua, O. M. Ntwaeaborwa, and H. C. Swart, "Latest development on pulsed laser deposited thin films for advanced luminescence applications," *Coatings*, vol. 10, no. 11, pp. 1–22, 2020.

[90] H. Angus Macleod, *Recent developments in deposition techniques for optical thin films and coatings*. Elsevier LTD., 2018.

[91] H. K. Raut, A. S. Nair, S. S. Dinachali, V. A. Ganesh, T. M. Walsh, and S. Ramakrishna, "Porous SiO_2 anti-reflective coatings on large-area substrates by electrospinning and their application to solar modules," *Sol. Energy Mater. Sol. Cells*, vol. 111, pp. 9–15, 2013.

[92] E. Taher, F.A., Abdeltwab, "Chemical Approaches for 1D Oxide Nanostructures, Nanomaterials Synthesis Design, Fabrication and Applications," *Micro Nano Technol.*, pp. 53–83, 2019.

[93] Y. Li, D., Xia, "Fabrication of titania nanofbers by electrospinning.," *Nano Lett.*, pp. 555–560, 2003.

[94] S. V. Eskin, I. D. Kosobudskiy, A. B. Zhimalov, N. M. Ushakov, D. M. Kulbatskiy, and S. V. German, "Antireflective coatings based on SiO_2 nanoparticles," *Inorg. Mater.*, vol. 48, no. 10, pp. 1006–1011, 2012.

[95] Y. Dimitriev, Y. Ivanova, and R. Iordanova, "ChemInform Abstract: History of Sol-Gel Science and Technology," *ChemInform*, vol. 40, no. 12, pp. 181–192, 2009.

[96] Y. Xu, W. H. Fan, Z. H. Li, D. Wu, and Y. H. Sun, "Antireflective silica thin films with super water repellence via a sol-gel process," *Appl. Opt.*, vol. 42, no. 1, p. 108, 2003.

[97] H. Tamon, T. Kitamura, and M. Okazaki, “Preparation of silica aerogel from TEOS,” *J. Colloid Interface Sci.*, vol. 197, no. 2, pp. 353–359, 1998.

[98] Ş. Toygun, G. K. Ğ. Lu, and Y. Kalpakli, no. 212, pp. 456–476, 2013.

[99] B. J. X. Zhang, S. Cai, D. You, L. Yan, H. Lv, X. Yuan, “Template free sol-gel preparation of superhydrophobic ORMOSIL films for double wavelength broadband antireflective coating,” *Adv. Funct. Mater.*, vol. 23, no. 25, pp. 4361–4365, 2013.

[100] D. Li, Y. Shan, F. Huang, and S. Ding, “Sol-gel preparation and characterization of SiO_2 coated VO_2 films with enhanced transmittance and high thermochromic performance,” *Appl. Surf. Sci.*, vol. 317, pp. 160–166, 2014.

[101] J. Philipavičius, I. Kazadojev, A. Beganskiene, A. Melninkaitis, V. Sirutkaitis, and A. Kareiva, “Hydrophobic antireflective silica coatings via sol-gel process,” *Medziagotyra*, vol. 14, no. 4, pp. 283–287, 2008.

[102] S. V. Es’Kin *et al.*, “Antireflecting coatings for glass based on monolayers of amorphous silica nanoparticles,” *Glas. Phys. Chem.*, vol. 39, no. 4, pp. 409–413, 2013.

[103] G. Womack, K. Isbilir, F. Lisco, G. Durand, A. Taylor, and J. M. Walls, “The performance and durability of single-layer sol-gel anti-reflection coatings applied to solar module cover glass,” *Surf. Coatings Technol.*, vol. 358, no. November 2018, pp. 76–83, 2019.

[104] G. C. N.-A. R. C. T. M. 2010 M. E. I. A. T. T. M. 2010 M. E. Bruer, “Luminescent, quantum dot-based anti-reflective coatings for crystalline silicon photovoltaics,” p. 116 p., 2010.

[105] M. Poté, “Dip Coating vs. Spin Coating,” pp. 1–9, 2016.

[106] H. Ijadpanah-Saravi, M. Zolfaghari, A. Khodadadi, and P. Drogui, “Synthesis, characterization, and photocatalytic activity of TiO_2–SiO_2 nanocomposites,” *Desalin. Water Treat.*, vol. 57, no. 31, pp. 14647–14655, 2016.

[107] S. D. Wang and J. Y. Wang, “Anti-reflective and superhydrophobic films prepared from a sol at different withdrawal speeds,” *Appl. Surf. Sci.*, vol. 476,

no. November 2018, pp. 1035–1048, 2019.

[108] Y. J. Acosta-Silva *et al.*, "Nanostructured CeO_2 thin films prepared by the sol-gel dip-coating method with anomalous behavior of crystallite size and bandgap," *J. Nanomater.*, vol. 2019, 2019.

[109] H. L. Yang, L. Hao, J. N. Wang, Z. N. Zhang, X. P. Liu, and L. J. Jiang, "Self-Cleaning and Anti-reflective Films for All-Glass Evacuated Tube Solar Collectors," *Energy Procedia*, vol. 69, no. January, pp. 226–232, 2015.

[110] Ö. Kesmez, E. Burunkaya, N. Kiraz, H. E. Çamurlu, M. Asiltürk, and E. Arpaç, "Effect of acid, water and alcohol ratios on sol-gel preparation of anti-reflective amorphous SiO_2 coatings," *J. Non. Cryst. Solids*, vol. 357, no. 16–17, pp. 3130–3135, 2011.

[111] S. Cai, Y. Zhang, H. Zhang, H. Yan, H. Lv, and B. Jiang, "Sol-gel preparation of hydrophobic silica antireflective coatings with low refractive index by base/acid two-step catalysis," *ACS Appl. Mater. Interfaces*, vol. 6, no. 14, pp. 11470–11475, 2014.

[112] D. N. Joshi, S. R. Atchuta, Y. Lokeswara Reddy, A. Naveen Kumar, and S. Sakthivel, "Super-hydrophilic broadband anti-reflective coating with high weather stability for solar and optical applications," *Sol. Energy Mater. Sol. Cells*, vol. 200, no. November 2018, 2019.

[113] G. Chen *et al.*, "Process study about silica anti-reflection coatings prepared by sol–gel method for cadmium telluride solar cells," *J. Mater. Sci.*, vol. 53, no. 22, pp. 15588–15599, 2018.

[114] B. Xia, J. Luo, Y. Li, B. Yang, S. Zhang, and B. Jiang, "Preparation of sponge-like porous SiO_2 antireflective coatings with excellent environment-resistance by an acid-catalysed sol-gel method," *RSC Adv.*, vol. 7, no. 43, pp. 26834–26838, 2017.

[115] A. S. Sarkın, N. Ekren, and Ş. Sağlam, "A review of anti-reflection and self-cleaning coatings on photovoltaic panels," *Sol. Energy*, vol. 199, no. June 2019, pp. 63–73, 2020.

[116] X. Lu *et al.*, “Antifogging and antireflective silica film and its application on solar modules,” *Surf. Coatings Technol.*, vol. 206, no. 6, pp. 1490–1494, 2011.

[117] M. C. Bautista and A. Morales, “Silica antireflective films on glass produced by the sol-gel method,” *Sol. Energy Mater. Sol. Cells*, vol. 80, no. 2, pp. 217–225, 2003.

[118] Y. Sun *et al.*, “A simple method to control the microstructure and properties of sol-gel silica antireflective coatings,” *RSC Adv.*, vol. 7, no. 51, pp. 31950–31959, 2017.

[119] M. K. Hedayati, M. Abdelaziz, C. Etrich, S. Homaeigohar, C. Rockstuhl, and M. Elbahri, “Broadband anti-reflective coating based on plasmonic nanocomposite,” *Materials (Basel).*, vol. 9, no. 8, pp. 1–9, 2016.

PUBLICATIONS FROM THE THESIS

Conference Papers

1. C. Yıldırım, M. Çelikbilek Ersundu, A. E. Ersundu, "Development of Sol-Gel Based Anti-Reflective Coatings for Glasses Used in Photovoltaic Systems", in International Conference on Engineering Technologies-ICENTE'20, Konya, 2020.